Robust Data-Driven Predictive Control for Unknown Linear Systems With Bounded Disturbances

Kaijian Hu and Tao Liu, *Member, IEEE*

***Abstract*—This article presents a robust data-driven predictive control (RDPC) framework for linear time-invariant (LTI) systems affected by bounded disturbances and measurement noise. Unlike traditional model-based approaches, the proposed method relies solely on input-state-output (ISO) data without requiring prior system identification. Given that multiple systems can be consistent with the collected data due to disturbances and noise, a set of all possible systems using quadratic matrix inequalities is constructed. The RDPC scheme is then formulated as an optimization problem that minimizes an upper bound on the control objective while ensuring robust constraint satisfaction for all systems in the set. Unlike the existing robust data-driven model predictive control methods based on behavioral system theory, the proposed method does not require the precollected data to satisfy the persistently exciting condition of a sufficiently high order. It only needs the stabilizability of the LTI system to be controlled. The proposed approach is further extended for systems where the state is unmeasurable. By reformulating the problem using an autoregressive exogenous model, a dynamic output feedback controller that leverages input–output data directly is designed. The effectiveness of the proposed methods is validated through a case study on an unstable batch reactor, demonstrating comparable performance to model-based robust MPC and data-driven MPC approaches while reducing conservatism and computational complexity.**

***Index Terms*—Bounded disturbances and noise, linear time-invariant (LTI) systems, quadratic matrix inequalities (QMIs), robust data-driven predictive control (RDPC).**

I. Introduction

MODEL predictive control (MPC) has become widely popular in both academic research and industrial applications due to its ability to determine optimal control inputs in real time by repeatedly solving an optimization problem based on predicted system trajectories [1]. However, one significant challenge in MPC is managing system disturbances, which can cause deviations between predicted and actual system behavior, potentially degrading control performance and even threatening system stability [2]. To mitigate this issue, several methods have been developed over the past few decades [3], [4], [5], [6], [7], including tube-based MPC [3], [4] and receding horizon H_∞ control [5]. These approaches generally require an accurate nominal system model, which can be derived from first principles or identified through system data [8]. However, obtaining such an accurate model is often challenging in practice.

In recent years, advancements in data science and the increased availability of system data have spurred interest in direct data-driven control [9], [10], [11]. This approach focuses on learning controllers directly from data for systems with unknown dynamics, thereby sidestepping the need for an explicit model. Data-driven predictive control schemes have also been proposed [12], [13], [14], [15], including data-driven model predictive control (DMPC), also known as data-enabled predictive control [12], [13], and its dimension reduction variant [15]. These methods have applications, such as optimal wide-area control for power systems [16] and speed control for synchronous motor drives [17].

However, the abovementioned methods rely on Willems' fundamental lemma [18], which requires precollected data to be noise-free and to satisfy the persistently exciting (PE) condition of a sufficiently high order to uniquely identify the behavior of linear time-invariant (LTI) systems. Consequently, these methods are primarily suited for deterministic LTI systems without disturbances and need precollected data that meet the PE condition.

In the presence of random disturbances or noisy measurement data, the precollected data may not satisfy Willems' lemma, making it challenging to determine the true system behavior accurately. To address this, regularization parameters have been incorporated into the DMPC scheme, forming a robust DMPC (RDMPC) scheme [12], [13]. These parameters help approximate the true system with noise data [12], and it has been shown that RDMPC can achieve practical stability with respect to noise levels [13]. Nevertheless, RDMPC still requires data that meet the PE condition, which can be difficult or costly to obtain, especially for unstable systems [19]. Recent advancements have attempted to relax this requirement by using multiple datasets [20] or new kernel structures for the Hankel matrix [21]. However, these methods either depend on the prediction horizon [20] or apply only to noise-free data [21]. Thus, the challenge of designing a robust data-driven predictive control (RDPC) scheme that does not require the

Received 31 August 2024; revised 10 February 2025; accepted 5 April 2025. Date of publication 14 April 2025; date of current version 29 September 2025. The work was supported in part by the Research Grants Council of the Hong Kong Special Administrative Region through the Early Career Scheme under Grant 27206021 and in part by the National Natural Science Foundation of China under Grant 62173287. Recommended by Associate Editor E. C. Kerrigan. *(Corresponding author: Tao Liu.)*

The authors are with the Department of Electrical and Electronic Engineering, The University of Hong Kong, Hong Kong SAR, China, and also with the HKU Shenzhen Institute of Research and Innovation, Shenzhen, China (e-mail: kjhu@eee.hku.hk; taoliu@eee.hku.hk).

Digital Object Identifier 10.1109/TAC.2025.3560697

1558-2523 © 2025 IEEE. All rights reserved, including rights for text and data mining, and training of artificial intelligence and similar technologies. Personal use is permitted, but republication/redistribution requires IEEE permission. See https://www.ieee.org/publications/rights/index.html for more information.

Authorized licensed use limited to: University of Science & Technology of China. Downloaded on October 13,2025 at 10:47:17 UTC from IEEE Xplore. Restrictions apply.

PE condition and can handle general LTI systems with unknown dynamics, disturbances, and measurement noise remains unresolved.

Recent related works offer potential solutions to address the issues mentioned earlier. The informativity framework [22] suggests that precollected data can still be informative for controller design, even if it does not suffice for system identification. The matrix S-lemma [23], [24] is a powerful tool that helps link the controller with the precollected data by eliminating unknown systems. This approach has been successfully applied in various data-driven control methods, such as state-feedback control [23] and H_∞ control [10], [25]. In addition, robust model predictive control (RMPC) [6] offers a method for dealing with model uncertainties by designing a time-varying state feedback controller to minimize an upper bound on the objective function for all possible systems.

Building on the informativity framework [22], [23], [24] and RMPC [6], this article proposes a new RDPC scheme for unknown LTI systems with unknown disturbances and measurement noise. Inspired by the work in [22], [23], and [24], we construct a set that includes all systems compatible with the precollected data. Following the approach in [6], we derive an upper bound for the predictive controller's objective function for all systems within this set and design a state feedback controller to minimize this upper bound at each time step. Our proposed method guarantees both internal stability and the prescribed H_∞ control performance of the closed-loop system.

Recent studies, such as [26], [27], and [28], have removed the requirement for input data to meet the PE condition by using input-state data. While the works in [26] and [28] focus on LTI systems without disturbances, the work in [27] extends this to systems with disturbances. However, the work in [27] does not account for measurement noise and only addresses predictive control problems related to input and state objectives and constraints. In practice, objective functions and constraints often involve system outputs, particularly when the system state is not measurable [12]. For specific LTI systems with known system matrices, this issue can be resolved by converting output-based functions into state-based functions. However, this approach may not be applicable to general LTI systems with unknown matrices. In addition, the work in [27] ensures only internal stability without addressing disturbance attenuation in the closed-loop system and relies on the state, which may not be measurable in practical applications [29]. Therefore, it is crucial to incorporate measurable outputs into the controller design instead of relying on unmeasurable states [30]. Our proposed RDPC scheme addresses these issues.

The primary contributions of this article are as follows.

1) We propose a new RDPC scheme for unknown LTI systems subject to bounded disturbances using noisy input-state-output (ISO) data, and we extend this method to systems with unmeasurable states using only noisy input–output (IO) data.
2) Our control method ensures both internal stability and the prescribed H_∞ control performance of the closed-loop system.
3) We utilize multiple datasets to construct the system set, resulting in a smaller set than one constructed using a single dataset.

The rest of this article is organized as follows. In Section II, we formulate the problem and provide some preliminaries. Section III presents the RDPC scheme for unknown LTI systems using ISO data. In Section IV, we extend the control scheme to systems with unmeasurable states using IO data. Section V includes simulations to demonstrate the effectiveness of the proposed method. Finally, Section VI concludes this article.

Notations: Let $\mathbb{R}$, $\mathbb{Z}$, $\mathbb{N}$, and $\mathbb{N}^+$ represent the sets of real numbers, integers, natural numbers, and positive integers, respectively. Let I_n denote the $n\times n$ identity matrix, and $0_{n\times m}$ denote the $n\times m$ zero matrix. The subscripts n and $n\times m$ will be omitted when the dimensions are clear from the context. For a matrix $M\in\mathbb{R}^{n\times m}$, $M^\top$ denotes its transpose, M^{-1} denotes its inverse if it is square and nonsingular, $\sigma_{\max}(M)$ represents its largest eigenvalue if all its eigenvalues are real, $M^\dagger$ denotes its pseudoinverse, $\ker(M)$ denotes its matrix kernel, and $\|M\|_2=\sqrt{\sigma_{\max}(M^\top M)}$ is its induced 2-norm. When referring to a symmetric matrix M, $M<0\,(M\leq 0)$ indicates that M is negative (semi)definite. The notation $\mathrm{diag}(M_1,\ldots,M_s)$ represents a block-diagonal matrix with matrices $M_1,\ldots,M_s$ on the diagonal. Given a signal $z(k):\mathbb{Z}\to\mathbb{R}^n$, $z(k)\in\mathcal{L}_2[0,T]$ denotes that the signals have finite energy over the interval $[0,T]$, i.e., $\sum_{k=0}^{T} z(k)^\top z(k)<\infty$, where $T\in\mathbb{N}$ satisfies $T<\infty$; define $z_{[k,k+L]}=[z(k),\ldots,z(k+L)]$, where $k\in\mathbb{Z}$ and $L\in\mathbb{N}$.

II. Preliminaries and Problem Formulation

Consider a discrete-time multiple-input and multiple-output LTI system

$$x_t(k+1)=A_t x_t(k)+B_t u(k)+\omega_d(k) \tag{1a}$$

$$y_t(k)=C_t x_t(k)+D_t u(k) \tag{1b}$$

where $u(k)\in\mathbb{R}^m$, $x_t(k)\in\mathbb{R}^n$, $y_t(k)\in\mathbb{R}^p$, and $\omega_d(k)\in\mathbb{R}^n$ are the system input, state, output, and unknown disturbance, respectively. The system matrices $A_t\in\mathbb{R}^{n\times n}$, $B_t\in\mathbb{R}^{n\times m}$, $C_t\in\mathbb{R}^{p\times n}$, and $D_t\in\mathbb{R}^{p\times m}$ are unknown but of known dimensions.

For simplicity, this article considers the measured output and the performance output to be the same. Therefore, the output equation is not only used to represent the system's measured output but also plays a crucial role in defining the performance output within the objective function. This dual role of the output equation is essential for ensuring that both the control objectives (e.g., minimizing output error) and constraints (e.g., output bounds) are incorporated into the control design.

Let $x(k)\in\mathbb{R}^n$ and $y(k)\in\mathbb{R}^p$ be the measured state and output, respectively, both corrupted by unknown but bounded noise

$$x(k)=x_t(k)+\delta_x(k)$$

$$y(k)=y_t(k)+\delta_y(k)$$

where $\delta_x(k)\in\mathbb{R}^n$ and $\delta_y(k)\in\mathbb{R}^p$ are the measurement noises.

The following assumptions, commonly used in robust data-driven control literature [23], [24], are made.

Assumption 1: The system dimensions m, n, and p are known, but the specific values of A_t, B_t, C_t, and D_t are unknown.

Assumption 2: The disturbance $\omega_d(k)$ and measurement noises $\delta_x(k)$ and $\delta_y(k)$ are bounded by

$$|\omega_{d,\iota}(k)|\leq\omega_{d,\iota,\max}\quad\forall\iota=1,\ldots,n \tag{2a}$$

$$|\delta_{x,\iota}(k)|\leq\delta_{x,\iota,\max}\quad\forall\iota=1,\ldots,n \tag{2b}$$

$$|\delta_{y,\iota}(k)|\leq\delta_{y,\iota,\max}\quad\forall\iota=1,\ldots,p \tag{2c}$$

Authorized licensed use limited to: University of Science & Technology of China. Downloaded on October 13,2025 at 10:47:17 UTC from IEEE Xplore. Restrictions apply.

for all $k \in \mathbb{N}$, where $\omega_{d,\iota}(k)$, $\delta_{x,\iota}(k)$, and $\delta_{y,\iota}(k)$ are the ιth entries of $\omega_d(k)$, $\delta_x(k)$, and $\delta_y(k)$, respectively, and $\omega_{\iota,\max}$, $\delta_{x,\iota,\max}$, and $\delta_{y,\iota,\max}$ are positive scalars. Furthermore, $\omega_d(k)$, $\delta_x(k)$, and $\delta_y(k)$ are assumed to be mutually independent.

Assumption 2 implies that the measurement noises $\delta_x(k)$ and $\delta_y(k)$ belong to $\mathcal{L}_2[0, T]$, meaning their energy remains finite over the given horizon. This condition aligns with common assumptions in robust control and H_∞ analysis, ensuring the well-posedness and stability of the closed-loop system. In practice, sensor noise and external disturbances are typically bounded in energy due to physical limitations.

Denote r as the number of precollected trajectories of the system (1), each of which has length T_j. Let $u_{j,[0,T_j-1]}$, $x_{j,[0,T_j]}$, and $y_{j,[0,T_j-1]}$, $j = 1,\ldots,r$, be the jth input, measured state, and measured output trajectories under unknown disturbances $\omega_{d,j,[0,T_j-1]}$ and measurement noises $\delta_{x,j,[0,T_j]}$ and $\delta_{y,j,[0,T_j-1]}$. We refer to each of these ISO trajectories as a dataset. For each dataset $j \in \mathscr{R} = \{1,\ldots,r\}$, define

$$U_j = [u_j(0), u_j(1), \ldots, u_j(T_j-1)] \tag{3a}$$
$$X_j = [x_j(0), x_j(1), \ldots, x_j(T_j-1)] \tag{3b}$$
$$X_{j,+} = [x_j(1), x_j(2), \ldots, x_j(T_j)] \tag{3c}$$
$$Y_j = [y_j(0), y_j(1), \ldots, y_j(T_j-1)] \tag{3d}$$
$$W_{d,j} = [\omega_{d,j}(0), \omega_{d,j}(1), \ldots, \omega_{d,j}(T_j-1)] \tag{3e}$$
$$\Delta_{x,j} = [\delta_{x,j}(0), \delta_{x,j}(1), \ldots, \delta_{x,j}(T_j-1)] \tag{3f}$$
$$\Delta_{x,j,+} = [\delta_{x,j}(1), \delta_{x,j}(2), \ldots, \delta_{x,j}(T_j)] \tag{3g}$$
$$\Delta_{y,j} = [\delta_{y,j}(0), \delta_{y,j}(1), \ldots, \delta_{y,j}(T_j-1)]. \tag{3h}$$

By substituting $x_t(k) = x(k) - \delta_x(k)$ and $y_t(k) = y(k) - \delta_y(k)$ into (1), the system can be rewritten in terms of measured states and outputs

$$\begin{aligned} x(k+1) = A_t x(k) + B_t u(k) + \omega_d(k) \\ + \delta_x(k+1) - A_t\delta_x(k) \end{aligned} \tag{4a}$$
$$y(k) = C_t x(k) + D_t u(k) + \delta_y(k) - C_t\delta_x(k). \tag{4b}$$

Then, the matrices defined in (3a)–(3h) satisfy

$$X_{j,+} = A_t X_j + B_t U_j + W_{d,j} + \Delta_{x,j,+} - A_t\Delta_{x,j} \tag{5a}$$
$$Y_j = C_t X_j + D_t U_j + \Delta_{y,j} - C_t\Delta_{x,j} \quad \forall j \in \mathscr{R}. \tag{5b}$$

The goal of this article is to design a predictive control scheme for the unknown system (1) using the precollected data (3a)–(3d). To simplify the analysis, define $\omega(k) = [\omega_d(k)^\top, \delta_y(k)^\top, \delta_x(k+1)^\top, \delta_x(k)^\top]^\top \in \mathbb{R}^q$ with $q = 3n + p$, $E_t = [I_n, 0_{n\times p}, I_n, -A_t]$, and $G_t = [0_{p\times n}, I_p, 0_{p\times n}, -C_t]$. Then, the system (4) can be rewritten as

$$x(k+1) = A_t x(k) + B_t u(k) + E_t\omega(k) \tag{6a}$$
$$y(k) = C_t x(k) + D_t u(k) + G_t\omega(k). \tag{6b}$$

It is important to note that E_t and G_t incorporate the unknown system matrices A_t and C_t, respectively, and that $\omega(k)$ in (6) represents both process disturbances and measurement noise from the original system (1). For simplicity, we refer to $\omega(k)$ as the disturbance throughout this article. This reformulation consolidates uncertainties into a single term, streamlining the analysis while preserving the impact of measurement noise. The explicit introduction of $\delta_x(k)$ and $\delta_y(k)$ in (1) differentiates true states and outputs from their measured counterparts, which is essential for constructing the system set and designing the controller. Without this distinction, the role of measurement noise in data collection and constraint formulation would be obscured.

Although (1) and (6) describe the same system, (6) is expressed in terms of noisy state and output measurements. Any controller designed using the measured state $x(k)$ or output $y(k)$ for (6) remains applicable to (1), despite the presence of noise. Thus, for clarity and notational simplicity, we adopt (6) as the system model in the subsequent analysis.

From the definition of $\omega(k)$, the bound conditions in (2a)–(2c) can be equivalently expressed as

$$|\omega_\iota(k)| \le \omega_{\iota,\max} \quad \forall \iota = 1,\ldots,q \quad \forall k \in \mathbb{N} \tag{7}$$

where $\omega_\iota(k)$ and $\omega_{\iota,\max}$ are the ιth entries of $\omega(k)$ and $\omega_{\max}$, respectively, with $\omega_{\max} = [\omega_{d,1,\max},\ldots,\omega_{d,n,\max},\delta_{y,1,\max},\ldots,\delta_{y,p,\max},\delta_{x,1,\max},\ldots,\delta_{x,n,\max},\delta_{x,1,\max},\ldots,\delta_{x,n,\max}]^\top$.

The bounded region of $\omega(k)$ forms a polyhedron, which can be conservatively approximated by an ellipsoid [31] as

$$\omega(k)^\top \Upsilon^{-1}\omega(k) \le 1$$

which is equivalent to

$$\omega(k)\omega(k)^\top \le \Upsilon \quad \forall k \in \mathbb{N} \tag{8}$$

where $\Upsilon = q\,\mathrm{diag}(\omega_{1,\max}^2,\ldots,\omega_{q,\max}^2) \in \mathbb{R}^{q\times q}$ is a positive-definite matrix.

If the system matrices A_t, B_t, C_t, and D_t were known, the predictive control problem could be formulated as the following RMPC optimization at each time step k [32]:

$$\min_{\substack{u(k+i|k),\\ i=0,\ldots,L-1}} \quad J(k) \tag{9a}$$
$$\text{s.t.} \quad \begin{aligned} x(k+1+i|k) = A_t x(k+i|k) + B_t u(k+i|k) \\ + E_t\omega(k+i) \end{aligned} \tag{9b}$$
$$\begin{aligned} y(k+i|k) = C_t x(k+i|k) + D_t u(k+i|k) \\ + G_t\omega(k+i) \end{aligned} \tag{9c}$$
$$x(k|k) = x(k) \tag{9d}$$
$$u(k+i|k) \in \mathbb{U}, y(k+i|k) \in \mathbb{Y}. \tag{9e}$$

The objective function in (9a) is defined as

$$J(k) = \max_{\substack{\omega(k+i)\in\Theta\\ i=0,\ldots,L-1}} \sum_{i=0}^{L-1} \|Q^{\frac{1}{2}} y(k+i|k)\|_2^2 + \|R^{\frac{1}{2}} u(k+i|k)\|_2^2 \tag{10}$$

where $Q \in \mathbb{R}^{p\times p}$ and $R \in \mathbb{R}^{m\times m}$ are positive-definite weight matrices; L is the prediction horizon; Θ is the set of all admissible disturbances satisfying (7); $x(k|k) = x(k)$ is the measured value of the system state at time k; $x(k+i|k)$ $\forall i = 1,\ldots,L-1$ and $y(k+i|k)$ $\forall i = 0,\ldots,L-1$ are the predicted values of the system state and output, respectively; $u(k+i|k)$ $\forall i = 0,\ldots,L-1$, are the optimal control inputs to be calculated, and only $u(k) = u(k|k)$ is applied to the system (6); $\omega(k+i) \in \Theta$ $\forall i = 0,\ldots,L-1$, represent the random disturbances; and $\mathbb{U}$ and $\mathbb{Y}$ are the sets of input and output constraints, respectively. The problem (9) can be solved by applying some existing RMPC schemes, e.g., those in [3], [32], and [33].

Authorized licensed use limited to: University of Science & Technology of China. Downloaded on October 13,2025 at 10:47:17 UTC from IEEE Xplore. Restrictions apply.

Since the initial state $x(k|k)$ in (9) is derived from noisy measurements, the stability analysis of the closed-loop system using (9) with (1) must account for both the process disturbance $\omega_d(k)$ and measurement noises $\delta_x(k)$ and $\delta_y(k)$. While (1) and (6) describe the same system, the latter consolidates these uncertainties into a single disturbance term, $\omega(k)$, simplifying the analysis. This does not alter the fact that the initial condition used in MPC is inherently noisy; rather, it allows us to formulate the problem in a more tractable manner. In addition, the internal stability properties of (1) and (6) remain identical when disturbances are absent, i.e., when $\omega_d(k) = 0$ in (1) and $\omega(k) = 0$ in (6). Therefore, to streamline the subsequent analysis while preserving the impact of measurement noise, we adopt (6) as the predictive model.

However, existing RMPC schemes cannot be directly applied to solve the MPC problem (9) since the matrices A_t, B_t, C_t, and D_t are unknown. Moreover, due to the presence of unknown disturbances, multiple systems could generate the same precollected ISO data, making it impossible to identify a unique nominal model [8] and then use it to solve (9).

To overcome the abovementioned issue, we formulate the following "min–max" optimization problem:

$$\min_{\substack{u(k+i|k),\\ i=0,\ldots,L-1}} \max_{(A,B,C,D)\in\Sigma} J(k) \tag{11a}$$

$$\text{s.t.} \quad x(k+1+i|k) = Ax(k+i|k) + Bu(k+i|k) + E\omega(k+i) \tag{11b}$$

$$y(k+i|k) = Cx(k+i|k) + Du(k+i|k) + G\omega(k+i) \tag{11c}$$

$$\text{(9d), (9e)} \tag{11d}$$

with $E = [I_n, 0_{n\times p}, I_n, -A]$ and $G = [0_{p\times n}, I_p, 0_{p\times n}, -C]$. To distinguish the real system matrices A_t, B_t, C_t, and D_t in (6), we use $A \in \mathbb{R}^{n\times n}$, $B \in \mathbb{R}^{n\times m}$, $C \in \mathbb{R}^{p\times n}$, and $D \in \mathbb{R}^{p\times m}$ to denote all possible system matrices that are consistent with the precollected data and use Σ to denote the set comprising all of these possible system matrices.

The objective of (11) is to determine the worst-case scenario for $J(k)$ among all systems in Σ and then minimize this worst-case value by appropriately designing control inputs. However, since Σ may contain infinite systems, solving (11) directly is computationally intractable [6].

To address this issue, we propose a new RDPC scheme for the unknown LTI system (6). This approach relies solely on the precollected data (3a)–(3d), eliminating the need for explicit system identification. It can be seen as a data-driven counterpart of the MPC scheme proposed in [6]. At each time step k, the RDPC scheme solves a data-driven optimization problem that minimizes an upper bound on the objective function $J(k)$ instead of directly minimizing its worst-case value. The control objectives are as follows.

1) Ensure that the system (6) is asymptotically stable when $\omega(k) = 0$ [i.e., (1) with $\omega_d(k) = 0$].
2) Guarantee that the closed-loop system with $x(0) = 0$ satisfies the H_∞ performance criterion

$$\sum_{k=0}^{T} \|z(k)\|_2^2 \leq \gamma^2 \sum_{k=0}^{T} \|\omega(k)\|_2^2 \tag{12}$$

for all $\omega(k) \in \mathcal{L}_2[0,T]$, where

$$z(k) = \begin{bmatrix} Q^{\frac{1}{2}} y(k) \\ R^{\frac{1}{2}} u(k) \end{bmatrix}$$

and $\gamma > 0$ is the disturbance attenuation level.

It is crucial to distinguish between the worst-case value and the upper bound of the objective function. The former represents the maximum achievable value of the objective function but is inherently unknown and cannot be computed exactly. In contrast, the upper bound provides a theoretical guarantee that the objective function does not exceed a specified limit. While this bound is generally more conservative, it remains analytically tractable. The proposed approach focuses on minimizing this upper bound rather than the worst-case value, ensuring robustness while maintaining computational efficiency. However, since the upper bound may not always be tight, some conservatism is introduced into the control design.

The gap between the true objective and its upper bound is influenced by several factors, including the conservatism of the system set, the prediction horizon, and the disturbance bound. A larger uncertainty set generally leads to a looser bound, increasing this gap. While the proposed method does not explicitly quantify this discrepancy, reducing the conservatism of the system set—for instance, by collecting more diverse datasets—can help mitigate it, which will be introduced later. Developing a precise theoretical characterization of this gap remains an open challenge and is an important direction for future research.

To improve the clarity, we will first introduce a predictive control scheme using ISO data under the assumption that the full system state is measurable. Then, we will extend this approach to the case where only IO data are available, allowing control of systems with unmeasurable states.

Before proceeding, we recall two mathematical results (i.e., the Schur complement lemma and matrix elimination lemma) that will be useful in subsequent derivations.

Lemma 1 (See [34]): Let $Q \in \mathbb{R}^{n\times n}$ and $P \in \mathbb{R}^{m\times m}$ be symmetric matrices, and $R \in \mathbb{R}^{n\times m}$ be an $n \times m$ matrix. The following three statements are equivalent.

1) $\begin{bmatrix} Q & R \\ R^\top & P \end{bmatrix} \leq 0.$
2) $Q < 0$ and $P - R^\top Q^{-1} R \leq 0$.
3) $P < 0$ and $Q - RP^{-1}R^\top \leq 0$.

In Lemma 1, the same equivalence holds if "$\leq$" is replaced with "$<$."

Lemma 2 (See [35]): Consider matrices $R \in \mathbb{R}^{n\times m}$ and $P \in \mathbb{R}^{n\times p}$, and a positive semidefinite matrix $\Phi \in \mathbb{R}^{p\times p}$. The following two statements are equivalent.

1) $RR^\top - P\Phi P^\top \leq 0$.
2) There exists a matrix $Q \in \mathbb{R}^{p\times m}$ such that $R = PQ$ and $QQ^\top - \Phi \leq 0$.

III. RDPC Scheme

In this section, we address the RDPC problem for the unknown LTI system (6) with measurable states using precollected ISO data. First, we construct the set Σ, which contains all possible system matrices that are consistent with the given data (3a)–(3d). Then, we propose a computationally tractable data-driven optimization problem as an alternative to the intractable

Authorized licensed use limited to: University of Science & Technology of China. Downloaded on October 13,2025 at 10:47:17 UTC from IEEE Xplore. Restrictions apply.

problem (11). Finally, the RDPC scheme is formulated by solving this new optimization problem at each time step.

A. Construction of the System Set

Define $W_j = [W_{d,j}^\top, \Delta_{y,j}^\top, \Delta_{x,j,+}^\top, \Delta_{x,j}^\top]^\top \forall j \in \mathscr{R}$. From (5), (6), (11b), and (11c), we have

$$X_{j,+} = AX_j + BU_j + EW_j \tag{13a}$$

$$Y_j = CX_j + DU_j + GW_j \quad \forall j \in \mathscr{R}. \tag{13b}$$

It is worth noting that in (13a) and (13b), the data matrices U_j, Y_j, X_j, and $X_{j,+}$ are known. However, the data matrices W_j and the system matrices A, B, C, and D are unknown.

Define $\Omega_j = \{W_j | \ (2a)-(2c) \ \ \forall k \in \mathcal{T}_j \text{ and } (2b) \text{ with } k = T_j\} \ \forall j \in \mathscr{R}$, where $\mathcal{T}_j = \{0, \ldots, T_j - 1\}$. Clearly, Ω_j represents the set of all possible values that the unknown matrix W_j can take.

For any given $W_j \in \Omega_j$, there exists at least one set of system matrices (A, B, C, D) satisfying (13a) and (13b). Since the true value of W_j is unknown and may take any value in Ω_j, there may exist multiple systems that are capable of generating the given ISO data (3a)–(3d). Since Ω_j is the minimum set containing all possible unknown matrices W_j, the set of all possible system matrices consistent with the given data can be defined as

$$\Sigma_j = \{(A, B, C, D) | (13a) \text{ and } (13b) \text{ and } W_j \in \Omega_j \text{ hold}\} \quad \forall j \in \mathscr{R}.$$

By definition, Σ_j must contain the true system, i.e., $(A_t, B_t, C_t, D_t) \in \Sigma_j \quad \forall j \in \mathscr{R}$.

To facilitate the design of the RDPC scheme, we incorporate the positive-definite weight matrices Q and R from the objective function $J(k)$ into the description of Σ_j. First, left-multiplying both sides of (13b) by $Q^{\frac{1}{2}}$ yields

$$Q^{\frac{1}{2}} Y_j = Q^{\frac{1}{2}} CX_j + Q^{\frac{1}{2}} DU_j + Q^{\frac{1}{2}} GW_j \forall j \in \mathscr{R}. \tag{14}$$

In addition, we introduce the following identity into Σ_j:

$$R^{\frac{1}{2}} U_j = 0_{m\times n} X_j + R^{\frac{1}{2}} U_j \quad \forall j \in \mathscr{R}. \tag{15}$$

Since (14) is equivalent to (13b), and (15) is an identity, the set Σ_j can be written as

$$\Sigma_j = \{(A, B, C, D) | (13a) \text{ and } (14) \text{ and } (15) \text{ and } W_j \in \Omega_j \text{ hold}\} \quad \forall j \in \mathscr{R}.$$

Substituting E and G defined right after (11) into (13a) and (14), respectively, and combining the resulting expressions with (15) give

$$[I_{n+p+m}, Z] H_j = [I_{n+p+m}, Z] \mathcal{G} W_j \quad \forall j \in \mathscr{R} \tag{16}$$

with $H_j = [X_{j,+}^\top, (Q^{\frac{1}{2}} Y_j)^\top, (R^{\frac{1}{2}} U_j)^\top, -X_j^\top, -U_j^\top]^\top$ and

$$Z = \begin{bmatrix} A & B \\ Q^{\frac{1}{2}} C & Q^{\frac{1}{2}} D \\ 0_{m\times n} & R^{\frac{1}{2}} \end{bmatrix}, \mathcal{G} = \begin{bmatrix} I_n & 0 & 0_{n\times m} & 0 & 0 \\ 0 & Q^{\frac{1}{2}} & 0 & 0 & 0 \\ I_n & 0 & 0 & 0 & 0 \\ 0 & 0 & 0 & -I_n & 0 \end{bmatrix}^\top. \tag{17}$$

Thus, the set Σ_j can be equivalently expressed as

$$\Sigma_j = \{(A, B, C, D) | (16) \text{ and } W_j \in \Omega_j \text{ hold}\} \quad \forall j \in \mathscr{R}. \tag{18}$$

Since Σ_j depends on the unknown disturbance matrix W_j, directly designing a controller based on Σ_j is challenging. To address this, we eliminate the dependence on W_j by leveraging its bounded nature to construct a new set $\tilde{\Sigma}_j$, where $\Sigma_j \subseteq \tilde{\Sigma}_j$.

As mentioned in Section II, the boundary of $\omega(k)$ can be outer approximated by an ellipsoid, i.e., (8), which implies

$$W_j W_j^\top \leq \Upsilon_{T_j} \quad \forall j \in \mathscr{R} \tag{19}$$

where $\Upsilon_{T_j} = T_j \Upsilon$. Define $\tilde{\Omega}_j = \{W_j | (19) \text{ holds}\} \forall j \in \mathscr{R}$. Using this, we redefine the system set as

$$\tilde{\Sigma}_j = \{(A, B, C, D) | (16) \text{ and } W_j \in \tilde{\Omega}_j \text{ hold}\} \quad \forall j \in \mathscr{R}.$$

Since (19) implies $\Omega_j \subseteq \tilde{\Omega}_j$, it follows that $\Sigma_j \subseteq \tilde{\Sigma}_j$. Consequently, the true system matrices satisfy $(A_t, B_t, C_t, D_t) \in \Sigma_j \subseteq \tilde{\Sigma}_j$, ensuring that any robust data-driven predictive controller designed for $\tilde{\Sigma}_j$ remains valid for the true system.

According to Lemma 2, (16) under (19) is equivalent to

$$[I_{n+p+m}, Z] H_j H_j^\top [I_{n+p+m}, Z]^\top \leq [I_{n+p+m}, Z] \mathcal{G} \Upsilon_{T_j} \mathcal{G}^\top [I_{n+p+m}, Z]^\top \quad \forall j \in \mathscr{R}$$

which is equivalent to

$$[I_{n+p+m}, Z] N_j [I_{n+p+m}, Z]^\top \leq 0 \quad \forall j \in \mathscr{R} \tag{20}$$

with $N_j = H_j H_j^\top - \mathcal{G} \Upsilon_{T_j} \mathcal{G}^\top$. Therefore, the set $\tilde{\Sigma}_j$ can be rewritten as

$$\tilde{\Sigma}_j = \{(A, B, C, D) | (20) \text{ holds}\} \quad \forall j \in \mathscr{R}.$$

To further refine the system set, we define

$$\tilde{\Sigma}^\star = \bigcap_{j=1}^{r} \tilde{\Sigma}_j. \tag{21}$$

Since each $\tilde{\Sigma}_j$ contains the true system, i.e., $(A_t, B_t, C_t, D_t) \in \tilde{\Sigma}_j$ for all $j \in \mathscr{R}$, the intersection $\tilde{\Sigma}^\star$ also contains the true system. Therefore, any RDPC scheme designed for all systems in $\tilde{\Sigma}^\star$ remains applicable to the true system. Moreover, the size of $\tilde{\Sigma}^\star$ may be smaller than any individual $\tilde{\Sigma}_j$, $j \in \mathscr{R}$. Consequently, in this article, we replace Σ in (11) with $\tilde{\Sigma}^\star$ to reduce conservatism.

Remark 1: The derivation of the quadratic matrix inequality (QMI) (20) introduces conservatism. This arises because we first approximate the disturbance bound using an outer ellipsoid (8) and then apply the constraint (19), which effectively enlarges the admissible disturbance set $\omega(k)$. As a result, we obtain $\Omega_j \subseteq \tilde{\Omega}_j$, leading to $\Sigma_j \subseteq \tilde{\Sigma}_j$, which in turn increases the number of systems considered in the controller design. This conservatism can be mitigated by tightening the bounds on Υ and Υ_{T_j}. Since Υ_{T_j} depends on both the data length T_j and Υ, it can be reduced by decreasing either parameter. However, if T_j is too short, the collected data may lack sufficient information to design an effective controller. To address this, we adopt an approach inspired by the work in [10], where multiple short datasets are used instead of a single long dataset to construct Σ. Similarly, the parameter Υ can be refined by approximating the disturbance bound using multiple ellipsoids, although this extension is omitted in this article for brevity.

Remark 2: The system set Σ_j is not countable in a discrete sense, as it consists of infinitely many systems satisfying the

Authorized licensed use limited to: University of Science & Technology of China. Downloaded on October 13,2025 at 10:47:17 UTC from IEEE Xplore. Restrictions apply.

QMI constraints. From (18), each $\Sigma_j\ \forall j \in \mathscr{R}$, is defined by a QMI. By expressing the system matrices as vectors, this QMI can be rewritten as a quadratic inequality, which defines a hyperellipsoid. Consequently, the volume of this hyperellipsoid provides a continuous measure of the size of Σ_j. Similarly, the volume of the intersecting hyperellipsoids within the same space can be used to quantify the size of the intersection set $\tilde{\Sigma}^\star$, as demonstrated in [36]. This characterization offers a geometric perspective on the system set's complexity and helps assess the conservatism of the constructed uncertainty set.

Remark 3: The study in [27] assumes that the disturbance sequence is bounded by $W_j W_j^\top \leq \Upsilon_j$, which is equivalent to (19) with $\Upsilon_j = \Upsilon_{T_j}$. However, in practical applications, it is often more feasible to estimate bounds for individual entries of $\omega(k)$ rather than for W_j as a whole. This is because $\omega(k)$ comprises the process disturbance $\omega_d(k)$ and the measurement noises $\delta_x(k)$ and $\delta_y(k)$, whose bounds are typically determined separately in practice. Therefore, in this article, we assume that each entry of $\omega(k)$ is bounded, as stated in Assumption 2, and derive (19) from the constraints (2a)–(2c). Furthermore, Alanwar et al. [37] considered disturbances represented by a zonotope [38]. The disturbance model used in this article can be seen as a special case of that representation. Extending our approach to accommodate more general disturbance structures will be explored in future work.

Remark 4: From the definition of $\tilde{\Sigma}^\star$, the size of $\tilde{\Sigma}^\star$ may decrease as the number of datasets increases. Hence, collecting more datasets may reduce the conservativeness of the controller designed based on $\tilde{\Sigma}^\star$. Besides collecting new trajectories, an alternative way is to generate more datasets from the existing trajectories. This is because a single trajectory can be divided into multiple trajectories of varying lengths. Since trajectories of different lengths can generate system sets with different sizes, the intersection of these sets is potentially smaller than the system set derived from a single trajectory, which is illustrated by an example in [36]. Suppose we have precollected s ISO trajectories of length one, denoted as $(u_{\jmath,[0,0]}, x_{\jmath,[0,1]}, y_{\jmath,[0,0]})$, $\jmath = 1,\dots,s$. For each trajectory $\jmath \in \mathscr{S} = \{1,\dots,s\}$, define four data matrices as follows:

$$X_\jmath = x_\jmath(0), X_{\jmath,+} = x_\jmath(1), Y_\jmath = y_\jmath(0), U_\jmath = u_\jmath(0). \quad (22)$$

Then, different datasets can be created by using different combinations of the data matrices (22), denoted as

$$U = [U_{\jmath_1}, U_{\jmath_2}, \dots, U_{\jmath_\ell}], X = [X_{\jmath_1}, X_{\jmath_2}, \dots, X_{\jmath_\ell}]$$
$$X_+ = [X_{\jmath_1,+}, X_{\jmath_2,+}, \dots, X_{\jmath_\ell,+}], Y = [Y_{\jmath_1}, Y_{\jmath_2}, \dots, Y_{\jmath_\ell}]$$

where the subscripts $\jmath_1, \jmath_2, \dots, \jmath_\ell \in \mathscr{S}$ with $\jmath_1 \neq \jmath_2 \neq \cdots \neq \jmath_\ell$ and $\ell \leq s$. It is worth noting that the sample time of data sequences U, X, X_+, and Y is discontinuous, which is similar to the combination of multiple datasets used for the extension of Willems' fundamental lemma [20]. Theoretically, there are $C(s,\ell) = \frac{s(s-1)\cdots(s-\ell+1)}{\ell(\ell-1)\cdots 1}$ different datasets of length ℓ. If we consider all datasets of length not greater than ℓ, we can create $\sum_{\imath=1}^{\ell} C(s,\imath)$ different datasets.

B. Optimization Problem

In this section, we formulate a new data-driven optimization problem as a computationally tractable alternative to (11). Inspired by the work in [6], rather than directly minimizing the worst-case value of the objective function in (11), we focus on minimizing its upper bound.

Before presenting the main results, similar to [10, Lemma 2], we propose the following lemma.

Lemma 3: Let $M, N_j \in \mathbb{R}^{(n+m)\times(n+m)}$, $j = 1,\dots,r$, be symmetric matrices. If there exist scalars $\alpha_j \geq 0$, $j = 1,\dots,r$, and $\beta > 0$ such that

$$M - \sum_{j=1}^{r} \alpha_j N_j \leq \begin{bmatrix} -\beta I_n & 0 \\ 0 & 0_{m\times m} \end{bmatrix}$$

then the inequality $[I, Z]M[I, Z]^\top < 0$ holds for all $Z \in \mathbb{R}^{n\times m}$ satisfying

$$[I, Z]N_j[I, Z]^\top \leq 0 \quad \forall j = 1,\dots,r.$$

Proof: The proof is straightforward and thus is omitted. ∎

Remark 5: Lemma 3 extends the "if" condition of the matrix S-lemma to multiple QMIs. However, extending the "only if" condition to multiple QMIs remains an open problem for future research. Nonetheless, Lemma 3 is sufficient for designing the RDPC scheme based on multiple datasets.

Practical systems often impose constraints on inputs and outputs, such as peak limits on individual entries [6], norm constraints [39], and linear inequality constraints [40]. Here, we consider peak constraints on each input and output, which can be expressed as

$$|u_\iota(k)| \leq u_{\iota,\max}, \quad \iota = 1,\dots,m \quad (24a)$$
$$|y_\iota(k)| \leq y_{\iota,\max}, \quad \iota = 1,\dots,p \quad (24b)$$

where $u_\iota(k)$ and $y_\iota(k)$ are the ιth elements of $u(k)$ and $y_t(k)$, respectively, and $u_{\iota,\max}$ and $y_{\iota,\max}$ are positive scalars. Other types of constraints can be handled in a similar manner.

To incorporate the output constraints into the controller design, knowledge of the row vectors C_ι and D_ι, $\iota = 1,\dots,p$, is required, where C_ι and D_ι denote the ιth rows of C and D, respectively. However, both C and D are unknown and cannot be uniquely determined from the precollected data due to measurement noise. To address this issue, we construct a set encompassing all possible values of C_ι and D_ι using the precollected data, following a similar approach as in Section III-A. For brevity, define $\mathscr{P} = \{1,\dots,p\}$ and $\mathscr{M} = \{1,\dots,m\}$.

Define $Z_{y_\iota} = [C_\iota, D_\iota]\ \forall \iota \in \mathscr{P}$. Following the procedure used to derive (20), we obtain the following QMIs:

$$[1, Z_{y_\iota}]N_{j,y_\iota}[1, Z_{y_\iota}]^\top \leq 0 \quad \forall \iota \in \mathscr{P}, j \in \mathscr{R} \quad (25)$$

where $N_{j,y_\iota} = H_{j,y_\iota} H_{j,y_\iota}^\top - \mathcal{G}_{y_\iota} \Upsilon_{T_j} \mathcal{G}_{y_\iota}^\top$, and $H_{j,y_\iota} = [Y_{j,\iota}^\top, -X_j^\top, -U_j^\top]^\top$ with $Y_{j,\iota}$ being the ιth row of Y_j. In addition, $\mathcal{G}_{y_\iota}$ is defined as

$$\mathcal{G}_{y_\iota} = \begin{bmatrix} 0_{1\times n} & e_\iota & 0_{1\times n} & 0_{1\times n} \\ 0_{n\times n} & 0 & 0 & I_n \\ 0_{m\times n} & 0 & 0 & 0 \end{bmatrix}$$

where e_ι is the ιth row of I_p.

Consequently, the set containing all possible row vectors C_ι and D_ι can be expressed as

$$\tilde{\Sigma}_{j,y_\iota} = \{(C_\iota, D_\iota) | (25) \text{ holds}\} \quad \forall \iota \in \mathscr{P}, j \in \mathscr{R}.$$

Authorized licensed use limited to: University of Science & Technology of China. Downloaded on October 13,2025 at 10:47:17 UTC from IEEE Xplore. Restrictions apply.

Similarly, the intersection set of all $\tilde{\Sigma}_{j,y_\iota}$ is defined as

$$\tilde{\Sigma}^\star_{y_\iota} = \bigcap_{j=1}^{r} \tilde{\Sigma}_{j,y_\iota} \quad \forall \iota \in \mathscr{P}.$$

The solution to the data-based optimization problem is presented in the following theorem.

Theorem 1: Consider the system (6) subject to the input and output constraints (24a) and (24b). Suppose Assumptions 1 and 2 hold. Given a group of sets of precollected ISO data $(u_{j,[0,T_j-1]}, x_{j,[0,T_j]}, y_{j,[0,T_j-1]})$, $j = 1,\ldots,r$, of (6), and a positive scalar γ, if there exist scalars $\bar{\eta}_k > \Delta\eta$ with $\Delta\eta = L\gamma^2\|\Upsilon\|_2$, $\bar{\alpha}_{j,k} = \bar{\alpha}_j(k) \geq 0$, $\bar{\beta}_k = \bar{\beta}(k) > 0$, $\tau_{j,\iota,k} = \tau_{j,\iota}(k) \geq 0$, and $\lambda_{\iota,k} = \lambda_\iota(k) > 0\, \forall j \in \mathscr{R}$ and $\iota \in \mathscr{P}$, a matrix $\bar{S}_k \in \mathbb{R}^{m\times n}$, and a positive-definite matrix $\bar{\Gamma}_k \in \mathbb{R}^{n\times n}$ such that the optimization problem (26) is feasible at time k

$$\min_{\substack{\bar{\eta}_k,\bar{\alpha}_{j,k},\bar{\beta}_k,\bar{S}_k,\\ \bar{\Gamma}_k,\tau_{j,\iota,k},\lambda_{\iota,k},\\ \forall j\in\mathscr{R} \quad \forall \iota\in\mathscr{P}}} \bar{\eta}_k$$

$$\text{s.t.} \quad \begin{bmatrix} -1 & \sqrt{\Delta\eta} & x(k|k)^\top \\ \sqrt{\Delta\eta} & -\bar{\eta}_k & 0 \\ x(k|k) & 0 & -\bar{\Gamma}_k \end{bmatrix} \leq 0 \tag{26a}$$

$$\bar{\mathcal{M}}_k - \sum_{j=1}^{r} \bar{\alpha}_{j,k}\mathcal{N}_j \leq \begin{bmatrix} -\bar{\beta}_k I_{n+p+m} & 0 \\ 0 & 0 \end{bmatrix} \tag{26b}$$

$$\begin{bmatrix} -u^2_{\iota,\max} & \bar{S}_{\iota,k} \\ \bar{S}^\top_{\iota,k} & -\bar{\Gamma}_k \end{bmatrix} \leq 0 \quad \forall \iota \in \mathscr{M} \tag{26c}$$

$$\bar{\mathcal{M}}_{y_\iota,k} - \sum_{j=1}^{r} \tau_{j,\iota,k}\mathcal{N}_{j,y_\iota} \leq \begin{bmatrix} -\lambda_{\iota,k} & 0 \\ 0 & 0 \end{bmatrix} \quad \forall \iota \in \mathscr{P} \tag{26d}$$

then $x(k|k)^\top \bar{\eta}_k \bar{\Gamma}_k^{-1} x(k|k) + L\gamma^2\|\Upsilon\|_2$ is an upper bound on the objective $J(k)$. Furthermore, the optimal state feedback controller that minimizes the upper bound is given by

$$u(k+i|k) = F_k x(k+i|k), i = 0,\ldots,L-1 \tag{27}$$

with $F_k = \bar{S}_k\bar{\Gamma}_k^{-1}$. In addition, the predicted inputs and outputs satisfy the constraints

$$|u_\iota(k+i|k)| \leq u_{\iota,\max} \quad \forall \iota \in \mathscr{M} \tag{28a}$$

$$|y_\iota(k+i|k)| \leq y_{\iota,\max} \quad \forall \iota \in \mathscr{P} \tag{28b}$$

for all $i = 0,\ldots,L-1$. Here, $\bar{\mathcal{M}}_k$ is defined as $\bar{\mathcal{M}}_k = \mathrm{diag}(\bar{\mathcal{Q}}_k, \bar{\mathcal{R}}_k)$ with

$$\bar{\mathcal{Q}}_k = \begin{bmatrix} -\bar{\Gamma}_k + \frac{\bar{\eta}_k}{\gamma^2}\tilde{E}\tilde{E}^\top & \frac{\bar{\eta}_k}{\gamma^2}\tilde{E}\tilde{G}^\top Q^{\frac{1}{2}} & 0 \\ \frac{\bar{\eta}_k}{\gamma^2}Q^{\frac{1}{2}}\tilde{G}\tilde{E}^\top & -\bar{\eta}_k I_p + \frac{\bar{\eta}_k}{\gamma^2}Q^{\frac{1}{2}}\tilde{G}\tilde{G}^\top Q^{\frac{1}{2}} & 0 \\ 0 & 0 & -\bar{\eta}_k I_m \end{bmatrix} \tag{29}$$

$$\bar{\mathcal{R}}_k = \begin{bmatrix} \bar{\Gamma}_k + \frac{1}{\gamma^2}\bar{\eta}_k I_n & \bar{S}_k^\top & 0 \\ \bar{S}_k & 0 & \bar{S}_k \\ 0 & \bar{S}_k^\top & -\bar{\Gamma}_k \end{bmatrix}$$

$$\tilde{E} = [I_n, 0_{n\times p}, I_n], \tilde{G} = [0_{p\times n}, I_p, 0_{p\times n}] \tag{30}$$

$\bar{S}_{\iota,k}$ is the ιth row of $\bar{S}_k$, $\bar{\mathcal{M}}_{y_\iota,k} = \mathrm{diag}(-y^2_{\iota,\max}, \bar{\mathcal{R}}_k)$, $\mathcal{N}_j = \mathrm{diag}(N_j, 0)$ with N_j being defined right after (20), and $\mathcal{N}_{j,y_\iota} = \mathrm{diag}(N_{j,y_\iota}, 0)$ with N_{j,y_ι} being defined right after (25).

Proof: The proof consists of three main steps. First, we establish that $x(k|k)^\top \bar{\eta}_k \bar{\Gamma}_k^{-1} x(k|k) + L\gamma^2\|\Upsilon\|_2$ serves as an upper bound on the objective $J(k)$. Next, we demonstrate that the designed controller minimizes this upper bound. Finally, we verify that the input and output constraints (28a) and (28b) hold if the optimization problem (26) is feasible.

To facilitate the proof, we first introduce the closed-loop system dynamics and a quadratic function. Substituting the state feedback controller (27) into (11b) and (11c), the closed-loop system evolves as

$$x(k+i+1|k) = \bar{A}_k x(k+i|k) + E\omega(k+i) \tag{31a}$$

$$y(k+i|k) = \bar{C}_k x(k+i|k) + G\omega(k+i) \tag{31b}$$

for $i = 0,\ldots,L-1$, where $\bar{A}_k = \bar{A}(k) = A + BF_k$ and $\bar{C}_k = \bar{C}(k) = C + DF_k\, \forall (A,B,C,D) \in \tilde{\Sigma}^\star$.

Define $P_k = \bar{\eta}_k\bar{\Gamma}_k^{-1}$ and consider the quadratic function

$$V(x(k+i|k)) = x(k+i|k)^\top P_k x(k+i|k). \tag{32}$$

Then, the difference between $V(x(k+i+1|k))$ and $V(x(k+i|k))$ is given by

$$\Delta V(x(k+i|k)) = x(k+i+1|k)^\top P_k x(k+i+1|k) - x(k+i|k)^\top P_k x(k+i|k). \tag{33}$$

Substituting (31a) into (33) gives

$$\Delta V(x(k+i|k)) = \xi^\top \begin{bmatrix} \bar{A}_k^\top P_k \bar{A}_k - P_k & \bar{A}_k^\top P_k E \\ E^\top P_k \bar{A}_k & E^\top P_k E \end{bmatrix} \xi \tag{34}$$

with $\xi = [x(k+i|k)^\top, \omega(k+i)^\top]^\top$.

Step 1—Upper Bound on the Objective Function: We will prove that $x(k|k)^\top \bar{\eta}_k \bar{\Gamma}_k^{-1} x(k|k) + L\gamma^2\|\Upsilon\|_2$ is an upper bound for $J(k)$ if the linear matrix inequality (LMI) (26c) is feasible. Applying Lemma 1 to (26c), we obtain

$$\bar{M}_k - \sum_{j=1}^{r} \bar{\alpha}_{j,k} N_j \leq \begin{bmatrix} -\bar{\beta}_k I_{n+p+m} & 0 \\ 0 & 0 \end{bmatrix} \tag{35}$$

where $\bar{M}_k = \begin{bmatrix} \bar{\mathcal{Q}}_k & 0 & 0 \\ 0 & \bar{\Gamma}_k + \frac{1}{\gamma^2}\bar{\eta}_k I_n & \bar{S}_k^\top \\ 0 & \bar{S}_k & \bar{S}_k\bar{\Gamma}_k^{-1}\bar{S}_k^\top \end{bmatrix}$.

By applying Lemma 3, we conclude that if (35) holds, then

$$[I_{n+p+m}, Z]\bar{M}_k[I_{n+p+m}, Z]^\top < 0 \tag{36}$$

for all Z such that $[I_{n+p+m}, Z]N_j[I_{n+p+m}, Z]^\top \leq 0\, \forall j \in \mathscr{R}$. According to the definition of the set $\tilde{\Sigma}^\star$ in (21), it follows that if the inequality (35) holds, then the inequality (36) holds for all systems in $\tilde{\Sigma}^\star$.

Substituting Z in (17), $\bar{\mathcal{Q}}_k$ in (29), and $F_k = \bar{S}_k\bar{\Gamma}_k^{-1}$, i.e., $\bar{S}_k = F_k\bar{\Gamma}_k$, into (36), and substituting $\bar{A}_k = A + BF_k$, $\bar{C}_k = C + DF_k$, $E = [\tilde{E}, -A]$, and $G = [\tilde{G}, -C]$ into the resulting expression yield

$$\mathrm{diag}(-\bar{\Gamma}_k, -\bar{\eta}_k I_p, -\bar{\eta}_k I_m)$$

Authorized licensed use limited to: University of Science & Technology of China. Downloaded on October 13,2025 at 10:47:17 UTC from IEEE Xplore. Restrictions apply.

$$-\begin{bmatrix}\bar{A}_k & E\\ Q^{\frac{1}{2}}\bar{C}_k & Q^{\frac{1}{2}}G\\ R^{\frac{1}{2}}F_k & 0_{m\times q}\end{bmatrix}\begin{bmatrix}-\bar{\Gamma}_k & 0\\ 0 & -\frac{\bar{\eta}_k}{\gamma^2}I_q\end{bmatrix}\begin{bmatrix}\bar{A}_k & E\\ Q^{\frac{1}{2}}\bar{C}_k & Q^{\frac{1}{2}}G\\ R^{\frac{1}{2}}F_k & 0_{m\times q}\end{bmatrix}^\top < 0. \quad (37)$$

Since $\mathrm{diag}(-\frac{1}{\bar{\eta}_k}\bar{\Gamma}_k, -\frac{1}{\gamma^2}I_q) < 0$ and $\mathrm{diag}(-\frac{1}{\bar{\eta}_k}\bar{\Gamma}_k, -I_p, -I_m) < 0$, multiplying both sides of (37) with $\frac{1}{\bar{\eta}_k}$ and applying Lemma 1 to the resulting expression twice give

$$\begin{bmatrix}\Phi & \bar{A}_k^\top P_k E + \bar{C}_k^\top QG\\ E^\top P_k \bar{A}_k + G^\top Q\bar{C}_k & E^\top P_k E + G^\top QG - \gamma^2 I_q\end{bmatrix} < 0$$

which is equivalent to

$$\xi^\top \begin{bmatrix}\Phi & \bar{A}_k^\top P_k E + \bar{C}_k^\top QG\\ E^\top P_k \bar{A}_k + G^\top Q\bar{C}_k & E^\top P_k E + G^\top QG - \gamma^2 I_q\end{bmatrix}\xi < 0 \quad (38)$$

for all $\xi \neq 0$, where $\Phi = \bar{A}_k^\top P_k \bar{A}_k - P_k + \bar{C}_k^\top Q\bar{C}_k + F_k^\top RF_k$.

Combining (34) with (38) yields

$$\Delta V(x(k+i|k)) + \xi^\top \begin{bmatrix}\bar{C}_k^\top Q\bar{C}_k + F_k^\top RF_k & \bar{C}_k^\top QG\\ G^\top Q\bar{C}_k & G^\top QG - \gamma^2 I_q\end{bmatrix}\xi < 0. \quad (39)$$

Substituting (31b) and the state feedback controller $u(k+i|k) = F_k x(k+i|k)$ into (39) gives

$$\Delta V(x(k+i|k)) + \|Q^{\frac{1}{2}}y(k+i|k)\|_2^2 + \|R^{\frac{1}{2}}u(k+i|k)\|_2^2 < \gamma^2\|\omega(k+i)\|_2^2. \quad (40)$$

Summing (40) from $i=0$ to $i=L-1$ gives

$$V(x(k+L|k)) - V(x(k|k)) + J(k) < \gamma^2\sum_{i=0}^{L-1}\|\omega(k+i)\|_2^2. \quad (41)$$

From (8), we have $\omega(k+i)\omega(k+i)^\top \leq \Upsilon$, which implies

$$\|\omega(k+i)\|_2^2 \leq \|\Upsilon\|_2. \quad (42)$$

Combining (42) with (41) gives

$$J(k) < -V(x(k+L|k)) + V(x(k|k)) + L\gamma^2\|\Upsilon\|_2. \quad (43)$$

Due to $V(x(k+L|k)) \geq 0$, (43) yields

$$J(k) < V(x(k|k)) + L\gamma^2\|\Upsilon\|_2. \quad (44)$$

Therefore, if the LMI (26c) is feasible, then $x(k|k)^\top\bar{\eta}_k\bar{\Gamma}_k^{-1} x(k|k) + L\gamma^2\|\Upsilon\|_2$ is an upper bound on $J(k)$. Furthermore, since $L\gamma^2\|\Upsilon\|_2$ is a constant determined by the prediction horizon and the disturbance bounds, the upper bound can be minimized by finding suitable $\bar{\eta}_k$ and $\bar{\Gamma}_k$ to minimize $V(x(k|k))$.

Step 2—Miminization by the Designed Controller: Applying Lemma 1 to (26b) gives

$$\begin{bmatrix}-1+\frac{\Delta\eta}{\bar{\eta}_k} & x(k|k)^\top\\ x(k|k) & -\bar{\Gamma}_k\end{bmatrix} \leq 0. \quad (45)$$

Define $\Lambda_k = \mathrm{diag}(\sqrt{\bar{\eta}_k}, \frac{1}{\sqrt{\bar{\eta}_k}})$. Left- and right-multiplying both sides of (45) with Λ_k, respectively, gives

$$\begin{bmatrix}-\bar{\eta}_k + \Delta\eta & x(k|k)^\top\\ x(k|k) & -\frac{1}{\bar{\eta}_k}\bar{\Gamma}_k\end{bmatrix} \leq 0. \quad (46)$$

By applying Lemma 1 to (46), we get

$$V(x(k|k)) = x(k|k)^\top\bar{\eta}_k\bar{\Gamma}_k^{-1}x(k|k) \leq \bar{\eta}_k - \Delta\eta. \quad (47)$$

Furthermore, the optimization problem (26) is convex, as its objective function (26a) is convex and the constraints (26c)–(26e) are expressed as LMIs. Thus, if (26) is feasible, a globally optimal solution exists that minimizes $\bar{\eta}_k$. From (47), minimizing $\bar{\eta}_k$ directly results in minimizing $V(x(k|k))$. Consequently, the upper bound $V(x(k|k)) + L\gamma^2\|\Upsilon\|_2$ is also minimized. This implies that if (26) is feasible at time k, the optimal solutions $\bar{S}_k$ and $\bar{\Gamma}_k$ minimize $\bar{\eta}_k$, meaning that the control gain matrix $F_k = \bar{S}_k\bar{\Gamma}_k^{-1}$ minimizes the upper bound.

Step 3—Satisfaction of Input and Output Constraints: At this step, we demonstrate that if (26b) and (26c) are feasible, then the input constraint (28a) and output constraint (28b) are satisfied, provided that LMIs (26d) and (26e) are also feasible.

We begin by proving that the input constraint (28a) holds under the feasibility of LMIs (26b)–(26d). Applying Lemma 1 to (26d) gives $\bar{S}_{\iota,k}\bar{\Gamma}_k^{-1}\bar{S}_{\iota,k}^\top - u_{\iota,\max}^2 \leq 0$, which implies

$$\|\bar{S}_{\iota,k}\bar{\Gamma}_k^{-\frac{1}{2}}\|_2 = \sqrt{\sigma_{\max}(\bar{S}_{\iota,k}\bar{\Gamma}_k^{-1}\bar{S}_{\iota,k}^\top)} \leq u_{\iota,\max}. \quad (48)$$

On the other hand, (40) can be rewritten as

$$x(k+i|k)^\top\bar{\eta}_k\bar{\Gamma}_k^{-1}x(k+i|k) \leq \bar{\eta}_k - \Delta\eta + \sum_{\jmath=0}^{i-1}\mu(k+\jmath|k) \quad (49)$$

with $\mu(k+\jmath|k) = -\|Q^{\frac{1}{2}}y(k+\jmath|k)\|_2^2 - \|R^{\frac{1}{2}}u(k+\jmath|k)\|_2^2 + \gamma^2\|\omega(k+\jmath)\|_2^2$.

Given that $\|\omega(k+\jmath)\|_2^2 \leq \|\Upsilon\|_2$ from (42), the upper bound on $\sum_{\jmath=0}^{i-1}\mu(k+\jmath|k)\ \forall i = 0,\ldots,L-1$, is

$$\sum_{\jmath=0}^{i-1}\mu(k+\jmath|k) \leq \gamma^2\sum_{\jmath=0}^{i-1}\|\omega(k+\jmath)\|_2^2 \leq \gamma^2\sum_{\jmath=0}^{L-2}\|\omega(k+\jmath)\|_2^2 \leq (L-1)\gamma^2\|\Upsilon\|_2. \quad (50)$$

Combining $\Delta\eta = L\gamma^2\|\Upsilon\|_2$, (49) and (50) gives

$$x(k+i|k)^\top\bar{\eta}_k\bar{\Gamma}_k^{-1}x(k+i|k) \leq \bar{\eta}_k - \gamma^2\|\Upsilon\|_2 \leq \bar{\eta}_k \quad (51)$$

for all $i = 0,\ldots,L-1$. Multiplying both sides of (51) by $\frac{1}{\bar{\eta}_k}$ and utilizing the definition of 2-norm yield

$$\|\bar{\Gamma}_k^{-\frac{1}{2}}x(k+i|k)\|_2 = \sqrt{\sigma_{\max}(x(k+i|k)^\top\bar{\Gamma}_k^{-1}x(k+i|k))} \leq 1 \quad (52)$$

for all $i = 0,\ldots,L-1$.

Further, combining (48) with (52) yields

$$\|\bar{S}_{\iota,k}\bar{\Gamma}_k^{-1}x(k+i|k)\|_2 \leq \|\bar{S}_{\iota,k}\bar{\Gamma}_k^{-\frac{1}{2}}\|_2\|\bar{\Gamma}_k^{-\frac{1}{2}}x(k+i|k)\|_2 \leq u_{\iota,\max} \quad (53)$$

Authorized licensed use limited to: University of Science & Technology of China. Downloaded on October 13,2025 at 10:47:17 UTC from IEEE Xplore. Restrictions apply.

for all $i = 0, \dots, L-1$. Substituting $u_\iota(k+i|k) = \bar{S}_{\iota,k}\bar{\Gamma}_k^{-1} x(k+i|k)$ into (53) gives

$$\|u_\iota(k+i|k)\|_2 \le u_{\iota,\max} \quad \forall i = 0, \dots, L-1. \tag{54}$$

Since $u_\iota(k+i|k)$ is a scalar, we have $\|u_\iota(k+i|k)\|_2 = |u_\iota(k+i|k)|$. Substituting it into (54) gives (28a). Thus, (28a) is satisfied if LMIs (26b)–(26d) are feasible.

Next, we prove that the output constraint (28b) holds under the feasibility of LMIs (26b), (26c), and (26e). Following a similar derivation from (35) to (36), we establish that if (26e) is feasible, then

$$[1, Z_{y_\iota}]M_{y_\iota,k}[1, Z_{y_\iota}]^\top < 0 \tag{55}$$

for any Z_{y_ι} satisfying $[1, Z_{y_\iota}]N_{j,y_\iota}[1, Z_{y_\iota}]^\top \le 0 \forall j \in \mathscr{R}$, where

$$M_{y_\iota,k} = \begin{bmatrix} -y_{\iota,\max}^2 & 0 & 0 \\ 0 & \bar{\Gamma}_k + \frac{1}{\gamma^2}\bar{\eta}_k I_n & \bar{S}_k^\top \\ 0 & \bar{S}_k & \bar{S}_k\bar{\Gamma}_k^{-1}\bar{S}_k^\top \end{bmatrix}.$$

Substituting $Z_{y_\iota} = [C_\iota, D_\iota]$ and $F_k = \bar{S}_k\bar{\Gamma}_k^{-1}$, i.e., $\bar{S}_k = F_k\bar{\Gamma}_k$, into (55) gives

$$\begin{bmatrix} C_\iota^\top \\ D_\iota^\top \end{bmatrix}^\top \begin{bmatrix} I_n & I_n \\ F_k & 0 \end{bmatrix} \begin{bmatrix} \bar{\Gamma}_k & 0 \\ 0 & \frac{\bar{\eta}_k}{\gamma^2} \end{bmatrix} \begin{bmatrix} I_n & I_n \\ F_k & 0 \end{bmatrix}^\top \begin{bmatrix} C_\iota^\top \\ D_\iota^\top \end{bmatrix} < y_{\iota,\max}^2$$

which is equivalent to

$$\left\| \begin{bmatrix} C_\iota^\top \\ D_\iota^\top \end{bmatrix}^\top \begin{bmatrix} I_n & I_n \\ F_k & 0 \end{bmatrix} \begin{bmatrix} \bar{\Gamma}_k^{\frac{1}{2}} & 0 \\ 0 & \frac{1}{\gamma}\sqrt{\bar{\eta}_k} \end{bmatrix} \right\|_2 < y_{\iota,\max}. \tag{56}$$

On the other hand, from $\|\omega(k+i)\|_2^2 \le \|\Upsilon\|_2$, we have $\|\delta_x(k+i)\|_2^2 \le \|\Upsilon\|_2$. Combining it with (51) gives

$$x(k+i|k)^\top\bar{\Gamma}_k^{-1}x(k+i|k) + \delta_x(k+i)^\top\frac{\gamma^2}{\bar{\eta}_k}\delta_x(k+i) \le 1$$

which implies

$$\left\| \begin{bmatrix} \bar{\Gamma}_k^{-\frac{1}{2}} & 0 \\ 0 & \frac{1}{\sqrt{\bar{\eta}_k}}\gamma \end{bmatrix} \begin{bmatrix} x(k+i|k) \\ -\delta_x(k+i) \end{bmatrix} \right\|_2 \le 1 \tag{57}$$

for all $i = 0, \dots, L-1$.

Combining (56) with (57) yields

$$\|(C_\iota + D_\iota F_k)x(k+i|k) - C_\iota\delta_x(k+i)\|_2 < y_{\iota,\max}$$

which together with the fact that $(C_\iota + D_\iota F_k)x(k+i|k) - C_\iota\delta_x(k+i)$ is a scalar, implies

$$|(C_\iota + D_\iota F_k)x(k+i|k) - C_\iota\delta_x(k+i)| < y_{\iota,\max} \tag{58}$$

for all $i = 0, \dots, L-1$.

Substituting $y_\iota(k+i|k) = (C_\iota + D_\iota F_k)x(k+i|k) - C_\iota \delta_x(k+i)$, i.e., ιth row of (31b) with $\delta_y(k+i) = 0$, into (58) gives the output constraint (28b). Thus, the output constraint (28b) is satisfied if LMIs (26b), (26c), and (26e) are feasible. ■

Notably, the measurement noise is incorporated in two critical ways in the proposed framework. First, it affects the construction of the system set. Specifically, the noisy IO data are used to define the system set, which introduces uncertainty in the representation of the system's dynamics. Second, at each time step k, the noisy measurements of the state $x(k)$ are used in the control law, specifically in the state feedback controller $u(k) = F_k x(k)$. This means that the measurement noise impacts the control inputs and, consequently, the system behavior at every step.

Remark 6: To establish that $V(x(k|k)) + L\gamma^2\|\Upsilon\|_2$ serves as an upper bound on $J(k)$, as stated in (44), it is essential to ensure that the QMI (36) incorporates the weight matrices Q and R from $J(k)$. This is achieved by embedding Q and R into the matrix Z, since the matrix M_k in (36) is fixed and does not inherently contain this information when $\tilde{G} = 0$. Furthermore, to derive the necessary conditions of (35), i.e., ensuring (36) holds under (20), it is crucial for the QMI constraints (20) and (36) to share the same matrix Z. This alignment is realized by incorporating (14) and (15) into (13), which justifies the use of Q and R in characterizing the set $\tilde{\Sigma}_j$ in (20).

Remark 7: For any given L, the term $L\gamma^2\|\Upsilon\|_2$ remains constant. Consequently, minimizing the upper bound $V(x(k|k)) + L\gamma^2\|\Upsilon\|_2$ is equivalent to minimizing $V(x(k|k))$. This implies that the optimization problem (26) effectively minimizes the upper bound on $J(k)$ for any finite prediction horizon ($L < \infty$).

Remark 8: For small prediction horizons L, an alternative approach to solving (11) is to directly optimize the sequence of predicted control inputs. This method provides more tunable parameters than using a single control gain matrix F_k, potentially improving control performance—an aspect that will be explored in future work. While modern solvers can handle large-scale optimization problems, their computational capacity is still influenced by factors, such as system order, input dimensionality, and constraint complexity. As L increases, the number of decision variables and constraints grows, leading to higher computational costs. Although solvers, such as IPOPT, can manage millions of variables, excessively large horizons may hinder real-time implementation. Identifying the precise boundary where optimization becomes impractical remains an open research question. Consequently, for large L, explicitly optimizing over predicted inputs becomes computationally demanding. In such cases, the proposed method offers a computational advantage by optimizing only the control gain matrix F_k, significantly reducing the number of decision variables while maintaining robust performance.

C. Control Scheme

This section presents the RDPC scheme, implemented in a receding horizon fashion by solving the optimization problem (26) iteratively. At each time step k, the measured state $x(k)$ is updated, and a new control gain matrix F_k is computed by solving (26). The proposed scheme is outlined in Algorithm 1.

The measured state $x(k)$ includes measurement noise and belongs to a subset of $\mathbb{R}^n$, which depends on the input and output constraints. Since these constraints are determined by the system set $\tilde{\Sigma}^\star$, characterizing the exact set of possible initial states remains challenging and will be explored in future work. However, if input and output constraints are disregarded, the initial state can take any value in $\mathbb{R}^n$.

To implement Algorithm 1, two fundamental issues must be addressed: (i) Ensuring that the optimization problem (26) remains feasible for all $k \in \mathbb{N}^+$. (ii) Verifying that the designed state feedback controller stabilizes the system (6).

Theorem 2 provides answers to these concerns.

Theorem 2: Consider the system (6) under Assumptions 1 and 2. Given a collection of precollected ISO datasets $(u_{j,[0,T_j-1]}, x_{j,[0,T_j]}, y_{j,[0,T_j-1]})$, $j = 1, \dots, r$, of (6), and a

Authorized licensed use limited to: University of Science & Technology of China. Downloaded on October 13,2025 at 10:47:17 UTC from IEEE Xplore. Restrictions apply.

Algorithm 1: RDPC Scheme With ISO Data.

Data: Input-state-output sequences
Select a positive scalar γ;
Initialize $k = 0$;
loop
  Set $x(k|k) = x(k)$ and solve (26);
  Compute control gain: $F_k = \bar{S}_k \bar{\Gamma}_k^{-1}$;
  Apply control input: $u(k|k) = F_k x(k|k)$;
  Update $k = k + 1$;
end loop

positive scalar γ, if the problem (26) is feasible at initial time $k = 0$, then the following holds:

i) the problem (26) remains feasible for all $k \in \mathbb{N}^+$;

ii) the system (6) with $\omega(k) = 0$ is asymptotically stabilized by the designed state feedback controller $u(k) = F_k x(k)$ with $F_k = \bar{S}_k \bar{\Gamma}_k^{-1}$; further, the closed-loop system with the initial condition $x(0) = 0$ has the H_∞ performance criterion (12).

Proof: To prove the statement (i), let $\bar{\eta}_k^*$, $\bar{\alpha}_{j,k}^*$, $\bar{\beta}_k^*$, $\bar{S}_k^*$, $\bar{\Gamma}_k^*$, $\tau_{j,\iota,k}^*$, and $\lambda_{\iota,k}^*$ $\forall j \in \mathscr{R}$ $\forall \iota \in \mathscr{P}$, denote the optimal solution to the problem (26) at time k. Define $P_k^* = \bar{\eta}_k^* \bar{\Gamma}_k^{*-1}$. The feasibility of (26) at time $k = 0$ implies that (26b)–(26e) hold at time $k = 0$.

Suppose that $(\bar{\eta}_0^*, \bar{\alpha}_{j,0}^*, \bar{\beta}_0^*, \bar{S}_0^*, \bar{\Gamma}_0^*, \tau_{j,\iota,0}^*, \lambda_{\iota,0}^* \forall j \in \mathscr{R} \forall \iota \in \mathscr{P})$ is a solution to (26) at $k = 0$. Applying the derivation process in (45)–(47) to (26b) at $k = 0$ gives

$$x(0|0)^\top P_0^* x(0|0) \leq \bar{\eta}_0^* - \Delta\eta. \tag{59}$$

Setting $k = 0$ and $i = 0$ in (40) gives

$$x(1|0)^\top P_0^* x(1|0) - x(0|0)^\top P_0^* x(0|0) < \mu(0|0) \tag{60}$$

with $\mu(0|0) = -\|Q^{\frac{1}{2}} y(0|0)\|_2^2 - \|R^{\frac{1}{2}} u(0|0)\|_2^2 + \gamma^2 \|\omega(0)\|_2^2$.

Since (60) holds for all systems in $\tilde{\Sigma}^\star$, including the true system (A_t, B_t, C_t, D_t), we have

$$x(1|1)^\top P_0^* x(1|1) - x(0|0)^\top P_0^* x(0|0) < \mu(0|0) \tag{61}$$

where $x(1|1) = (A_t + B_t F_0^*) x(0|0) + E_t \omega(0)$ with $F_0^* = \bar{S}_0^* \bar{\Gamma}_0^{*-1}$. Combining (61) with (59) gives

$$\begin{aligned} &x(1|1)^\top P_0^* x(1|1) \\ &< x(0|0)^\top P_0^* x(0|0) + \mu(0|0) \leq \bar{\eta}_0^* - \Delta\eta + \mu(0|0). \end{aligned} \tag{62}$$

Define $\tilde{\eta} = \eta_0^* + \mu(0|0)$. The inequality (62) becomes

$$x(1|1)^\top P_0^* x(1|1) \leq \tilde{\eta} - \Delta\eta. \tag{63}$$

Therefore, the LMI (26b) is feasible at time $k = 1$ by choosing $\bar{\Gamma}_1 = \bar{\Gamma}_0^*$ and $\bar{\eta}_1 = \tilde{\eta}$.

When only considering LMIs (26c)–(26e), their feasible solution space remains the same for all times $k \in \mathbb{N}$ as these LMIs only rely on the precollected data. Therefore, they remain feasible at $k = 1$ by setting $\bar{\alpha}_{j,1} = \bar{\alpha}_{j,0}^*$, $\bar{\beta}_1 = \bar{\beta}_0^*$, $\bar{S}_1 = \bar{S}_0^*$, $\bar{\Gamma}_1 = \bar{\Gamma}_0^*$, $\tau_{j,\iota,1} = \tau_{j,\iota,0}^*$, and $\lambda_{\iota,1} = \lambda_{\iota,0}^* \forall j \in \mathscr{R}, \iota \in \mathscr{P}$.

Since both (26b) and (26c) are feasible at time $k = 1$ by choosing $\bar{\eta}_1 = \tilde{\eta}$, $\bar{\alpha}_{j,1} = \bar{\alpha}_{j,0}^*$, $\bar{\beta}_1 = \bar{\beta}_0^*$, $\bar{S}_1 = \bar{S}_0^*$, $\bar{\Gamma}_1 = \bar{\Gamma}_0^*$, $\tau_{j,\iota,1} = \tau_{j,\iota,0}^*$, and $\lambda_{\iota,1} = \lambda_{\iota,0}^*$ $\forall j \in \mathscr{R}, \iota \in \mathscr{P}$, (26) is feasible at $k = 1$. Repeating this process proves that if (26) is feasible at $k = 0$, then it remains feasible for all $k \in \mathbb{N}^+$. This completes the proof of statement (i).

To prove (ii), consider the Lyapunov function candidate

$$\bar{V}(x(k)) = x(k)^\top P_k^* x(k). \tag{64}$$

Generalizing (62) to any k yields

$$x(k+1)^\top P_k^* x(k+1) < x(k)^\top P_k^* x(k) + \mu(k) \tag{65}$$

where $\mu(k) = -\|Q^{\frac{1}{2}} y(k)\|_2^2 - \|R^{\frac{1}{2}} u(k)\|_2^2 + \gamma^2 \|\omega(k)\|_2^2$.

Since P_{k+1}^* is the optimal solution to (26) at $k + 1$, we have

$$x(k+1)^\top P_{k+1}^* x(k+1) \leq x(k+1)^\top P_k^* x(k+1). \tag{66}$$

Combining (65) and (66) gives

$$\begin{aligned} &x(k+1)^\top P_{k+1}^* x(k+1) - x(k)^\top P_k^* x(k) \\ &< -\|Q^{\frac{1}{2}} y(k)\|_2^2 - \|R^{\frac{1}{2}} u(k)\|_2^2 + \gamma^2 \|\omega(k)\|_2^2. \end{aligned} \tag{67}$$

If $\omega(k) = 0$, then the inequality (67) becomes

$$\bar{V}(x(k+1)) - \bar{V}(x(k)) < -\|Q^{\frac{1}{2}} y(k)\|_2^2 - \|R^{\frac{1}{2}} u(k)\|_2^2. \tag{68}$$

Since $\bar{V}(x(k)) > 0$ and $\bar{V}(x(k+1)) - \bar{V}(x(k)) < 0$ for all $x(k) \neq 0$, the system (6) with $\omega(k) = 0$ is asymptotically stabilized by the designed state feedback controller.

Finally, for $\omega(k) \neq 0$ with $x(0) = 0$ and $z(k) = [(Q^{\frac{1}{2}} y(k))^\top, (R^{\frac{1}{2}} u(k))^\top]^\top$, summing (67) from $k = 0$ to $k = T$ with $T \in \mathbb{N}$ and $T < \infty$ establishes the H_∞ performance (12). This concludes the proof of (ii). ∎

Remark 9: Unlike the RMPC schemes in [3] and [6], our approach does not require knowledge of a nominal system model. Instead, it relies solely on collected data, making it both practical and advantageous. In addition, compared to [3], our method adopts a different strategy for handling bounded disturbances in LTI systems. Specifically, we construct a set encompassing all possible system realizations induced by disturbances and minimize the upper bound of the objective function $J(k)$ over this set. In contrast, Mayne et al. [3] employed a nominal system model and ensured that the uncertain predicted input-state trajectory remains within a sequence of constraint sets. Moreover, our method is inspired by the work in [6], which addresses uncertainty but does not explicitly consider disturbances.

Remark 10: Compared to the RDMPC schemes in [12] and [13], which leverage Willems' fundamental lemma, our method offers two notable advantages. First, it imposes no requirement on the length T_j of the continuously sampled data (3a)–(3d), as discussed in Remark 4. In contrast, RDMPC schemes rely on Hankel matrices, which require the data length to be at least the order of the Hankel matrix. Furthermore, these schemes demand full row rank (i.e., the PE condition) and a sufficiently large order relative to the prediction horizon. This highlights that our method simplifies data collection, particularly for unstable systems [19]. Second, our approach does not require system controllability; it only implicitly assumes stabilizability, as (26) would be infeasible otherwise.

Remark 11: The data-driven min–max MPC method in [27] also leverages the data informativity framework and, in some cases, addresses similar control problems. However, our approach introduces several key distinctions and extensions. First, our formulation explicitly accounts for both process disturbances and measurement noise, whereas the work in [27] primarily considers process disturbances. This distinction enhances

Authorized licensed use limited to: University of Science & Technology of China. Downloaded on October 13,2025 at 10:47:17 UTC from IEEE Xplore. Restrictions apply.

the practical applicability of our method in noisy environments. Second, while the work in [27] ensures internal closed-loop stability, our approach further guarantees the prescribed H_∞ performance (12), offering robustness against worst-case disturbances. Third, our method employs a more general IO-based objective function (10), whereas the work in [27] adopts an input-state-based objective function given by

$$\tilde{J}(k) = \sum_{i=0}^{L-1} \|\tilde{Q}^{\frac{1}{2}}\tilde{x}(k+i|k)\|_2^2 + \|R^{\frac{1}{2}}u(k+i|k)\|_2^2 \tag{69}$$

where $\tilde{Q} \in \mathbb{R}^{n\times n} > 0$ and $\tilde{x}(k+i+1|k) = A\tilde{x}(k+i|k) + Bu(k+i|k)$ with $\tilde{x}(k|k) = x_t(k)$. Unlike (69), which is based on the nominal system (11b) without disturbances [i.e., (11b) with $\omega(k) = 0$], our objective function (10) accounts for the actual system dynamics, incorporating disturbance effects. This fundamental difference enables our method to provide explicit H_∞ performance guarantees. In addition, when $\omega(k) = 0$, our IO-based objective function (10) simplifies to the input-state-based formulation (69). However, the reverse does not generally hold unless the system matrices C_t and D_t are known and satisfy $C_t^\top QC_t > 0$ with $D_t = 0$.

Remark 12: The RDPC scheme in [37] also accounts for both measurement noise and process disturbances but differs from our approach in three key aspects. First, it requires input data to satisfy the PE condition, similar to the RDMPC schemes in [12] and [13], as noted in Remark 10. Second, it considers only an input-state-based objective function, similar to [27], as discussed in Remark 11. Third, it requires computing the reachable set at each prediction horizon step, a computationally intensive step that our proposed method avoids.

Remark 13: The RDPC schemes proposed in [26] and [28] can be viewed as special cases of our approach. These schemes assume no disturbances or measurement noise and rely on a single dataset, i.e., $\omega_d(k) = 0, \delta_x(k) = 0, \delta_y(k) = 0$, and $r = 1$. In addition, the method in [26] considers only an input-state-based objective function, which has similar issues, as discussed in Remark 11.

Remark 14: A potential limitation of our method arises from the influence of disturbances $\omega(k)$, which make it difficult to identify a unique system from the precollected data. As discussed in Section III-A, the set $\tilde{\Sigma}^\star$ contains all systems consistent with the data, and the proposed controller is designed to accommodate all such systems. Consequently, the solution to the data-driven optimization problem (26) is generally more conservative compared to solving (9) when the system model is known, as it must ensure stability and performance across all possible systems in $\tilde{\Sigma}^\star$. The performance gap between the proposed method and the model-based approach is primarily determined by the size of $\tilde{\Sigma}^\star$. A larger system set results in a more conservative controller, potentially leading to a greater gap in performance. To mitigate this, multiple datasets can be leveraged to refine $\tilde{\Sigma}^\star$ and improve control efficiency, as highlighted in Remark 4. Investigating additional techniques to reduce conservatism and further close this performance gap remains an important direction for future research.

Remark 15: When $D_t = 0$, the system output at time k is directly available, allowing for a tighter upper bound on $\sum_{j=0}^{i-1}\mu(k+j|k)$ compared to (50). Specifically, it can be computed as $\delta_k = -\|Q^{\frac{1}{2}}y(k)\|_2^2 + L\gamma^2\|\Upsilon\|_2$. We define $\Delta\eta = \delta_k$ if $\delta_k > 0$, and $\Delta\eta = 0$ otherwise, incorporating this definition into (26b). This adjustment reduces conservatism and enables the design of a less conservative state feedback controller when $D_t = 0$, as implemented in Algorithm 1.

Remark 16: The implementation of Algorithm 1 requires selecting parameters, such as the prediction horizon L, the disturbance attenuation level γ, the number of datasets r, and the dataset lengths $T_j, \forall j \in \mathscr{R}$, on a case-by-case basis. These parameters significantly impact control performance. First, the prediction horizon L determines the length of the predicted IO trajectory that satisfies constraints. According to Theorem 1, since $\bar{\eta}_k \geq L\gamma^2\|\Upsilon\|_2$, increasing L reduces the feasible region of $\bar{\eta}_k$, resulting in a more conservative controller. Second, γ influences the attenuation of disturbances $\omega(k)$ in the closed-loop system. A smaller γ reduces disturbance effects, as seen in (12), but also increases controller conservatism, as reflected in (26c). Third, r and T_j impact the size of the system set $\tilde{\Sigma}^\star$. Increasing r reduces $\tilde{\Sigma}^\star$, leading to a less conservative controller but higher computational complexity [36]. In addition, increasing T_j may either enlarge or shrink $\tilde{\Sigma}_j$ [36], making it beneficial to use multiple short datasets, as recommended in Remark 4.

Remark 17: Since this study considers system (6) with unknown matrices (A_t, B_t, C_t, D_t), the output constraints are formulated without explicit knowledge of C_t and D_t. However, the proposed method can be easily adapted to cases where C_t and D_t are known, allowing direct computation of the output via the output equation instead of relying on output measurements. Furthermore, if the matrix $\Xi = \begin{bmatrix} X_1, \dots, X_r \\ U_1, \dots, U_r \end{bmatrix}$ has full row rank, then C_ι and D_ι can be uniquely determined from $Y_{j,\iota} = C_\iota X_j + D_\iota U_j \ \forall j \in \mathscr{R}$. Specifically, $[C_\iota, D_\iota] = Y_\iota \Xi^\top(\Xi\Xi^\top)^{-1}$, where Y_ι is the ιth row of $[Y_1, \dots, Y_r]$. In this case, $\tilde{\Sigma}^\star_{y_\iota}$ reduces to a singleton containing the true values of $C_{t,\iota}$ and $D_{t,\iota}$, the ιth rows of C_t and D_t, respectively. As a result, the output constraints (28b) with known C_t and D_t can be directly enforced using the proposed method.

Remark 18: The feasibility of (26) at $k = 0$ is crucial to the proposed control method and depends on the quality of the precollected data. Unlike methods requiring PE condition, our approach does not impose such conditions but relies on data sufficiently constraining $\tilde{\Sigma}^\star$. However, measurement noise and disturbances introduce uncertainties, making it difficult to derive explicit feasibility conditions. In practice, feasibility can often be improved by increasing the number or diversity of collected trajectories. Studying formal conditions for guaranteed feasibility is an important direction for future research.

IV. Extension to IO Case

In practical applications, system states may not always be measurable. To address this limitation, this section develops an RDPC scheme that relies solely on IO data. We consider an LTI system modeled using an autoregressive exogenous (ARX) representation

$$\begin{aligned} y_t(k) &= \mathcal{A}_{1t}y_t(k-1) + \cdots + \mathcal{A}_{n_o t}y_t(k-n_o) \\ &\quad + \mathcal{B}_{1t}u(k-1) + \cdots + \mathcal{B}_{n_c t}u(k-n_c) + \nu(k) \end{aligned} \tag{70}$$

where $u(k) \in \mathbb{R}^m$ and $y_t(k) \in \mathbb{R}^p$ denote the system input and output, respectively, while $\nu(k) \in \mathbb{R}^p$ represents an unknown disturbance. The system matrices $\mathcal{A}_{it} \in \mathbb{R}^{p\times p}$ and $\mathcal{B}_{it} \in \mathbb{R}^{p\times m}$, for $i = 1, \dots, n_o$ and $i = 1, \dots, n_c$, are unknown. The measured output $y(k)$ is corrupted by measurement noise $\delta_y(k)$, i.e., $y(k) = y_t(k) + \delta_y(k)$.

Authorized licensed use limited to: University of Science & Technology of China. Downloaded on October 13,2025 at 10:47:17 UTC from IEEE Xplore. Restrictions apply.

Similar to Assumption 2, we impose the following boundedness condition on $\nu(k)$ and $\delta_y(k)$.

Assumption 3: The disturbance $\nu(k)$ and measurement noise $\delta_y(k)$ satisfy

$$|\nu_\iota(k)| \leq \nu_{\iota,\max} \quad \forall \iota = 1,\ldots,p \tag{71a}$$

$$|\delta_{y,\iota}(k)| \leq \delta_{y,\iota,\max} \quad \forall \iota = 1,\ldots,p \tag{71b}$$

for all $k \in \mathbb{N}$, where $\nu_\iota(k)$ and $\delta_{y,\iota}(k)$ are the ιth elements of $\nu(k)$ and $\delta_y(k)$, respectively, and $\nu_{\iota,\max}$ and $\delta_{y,\iota,\max}$ are positive scalars.

To apply the predictive control framework from Section III, we first transform the ARX model (70) into an equivalent state-space representation. This representation maintains the same IO relationship as the original ARX model. The state of the system is constructed using the historical input and output of (70), i.e.,

$$\begin{aligned}\hat{x}_t(k) = [&u(k-n_c)^\top, \ldots, u(k-1)^\top,\\ &y_t(k-n_o)^\top, \ldots, y_t(k-1)^\top]^\top \in \mathbb{R}^{\hat{n}}\end{aligned} \tag{72}$$

where $\hat{n} = n_c m + n_o p$. The corresponding state-space model is then given by

$$\hat{x}_t(k+1) = \hat{A}_t \hat{x}_t(k) + \hat{B}_t u(k) + \hat{\mathcal{E}}_t \nu(k) \tag{73a}$$

$$y_t(k) = \hat{C}_t \hat{x}_t(k) + \hat{D}_t u(k) + \nu(k) \tag{73b}$$

where

$$\hat{A}_t = \left[\begin{array}{cc|cc} 0 & I_{(n_c-1)m} & \multicolumn{2}{c}{\multirow{2}{*}{$0_{n_c m \times n_o p}$}} \\ 0_{m\times m} & 0 & & \\ \hline \multicolumn{2}{c|}{0_{(n_o-1)p \times n_c m}} & 0 & I_{(n_o-1)p} \\ \mathcal{B}_{n_c t} \ \ \ldots & \mathcal{B}_{1t} & \mathcal{A}_{n_o t} \ \ \ldots & \mathcal{A}_{1t} \end{array}\right]$$

$$\hat{B}_t = [0_{m\times(n_c-1)m}, I_m, 0_{m\times n_o p}]^\top, \hat{\mathcal{E}}_t = [0_{p\times(\hat{n}-p)}, I_p]^\top \tag{74}$$

$$\hat{C}_t = [\mathcal{B}_{n_c t}, \ldots, \mathcal{B}_{1t}, \mathcal{A}_{n_o t}, \ldots, \mathcal{A}_{1t}], \hat{D}_t = 0. \tag{75}$$

By substituting $y_t(k) = y(k) - \delta_y(k)$ into (73), we obtain the following system, which explicitly accounts for measurement noise:

$$\hat{x}(k+1) = \hat{A}_t \hat{x}(k) + \hat{B}_t u(k) + \hat{E}_t \hat{\omega}(k) \tag{76a}$$

$$y(k) = \hat{C}_t \hat{x}(k) + \hat{D}_t u(k) + \hat{G}_t \hat{\omega}(k) \tag{76b}$$

where $\hat{x}(k) = [u(k-n_c)^\top, \ldots, u(k-1)^\top, y(k-n_o)^\top, \ldots, y(k-1)^\top]^\top$, $\hat{\omega}(k) = [\nu(k)^\top, \delta_y(k-n_o)^\top, \ldots, \delta_y(k)^\top]^\top \in \mathbb{R}^{\hat{q}}$ with $\hat{q} = (n_o+2)p$, $\hat{E}_t = [\hat{\mathcal{E}}_t, I_{\hat{n}}, -\hat{A}_t][\mathcal{L}_1^\top, \mathcal{L}_2^\top]^\top$, and $\hat{G}_t = [I_p, 0_{p\times(\hat{n}-p)}, I_p, -\hat{C}_t][\mathcal{L}_1^\top, \mathcal{L}_2^\top]^\top$ with

$$\mathcal{L}_1 = \begin{bmatrix} I_p & 0 \\ 0 & E_{1t} \end{bmatrix}, \mathcal{L}_2 = [0_{\hat{n}\times p}, E_{2t}]$$

$$E_{1t} = \left[\begin{array}{c:c} 0_{n_c m\times p} & 0 \\ \hdashline 0 & I_{n_o p} \end{array}\right], E_{2t} = \left[\begin{array}{c:c} 0 & 0_{n_c m\times p} \\ \hdashline I_{n_o p} & 0 \end{array}\right].$$

Define $\hat{\omega}_{\max} = [\nu_{\max}^\top, \delta_{y,\max}^\top, \ldots, \delta_{y,\max}^\top]^\top \in \mathbb{R}^{\hat{q}}$ with $\nu_{\max} = [\nu_{1,\max}, \ldots, \nu_{p,\max}]^\top$ and $\delta_{y,\max} = [\delta_{y,1,\max}, \ldots, \delta_{y,p,\max}]^\top$. Similar to (8), the disturbance bound is approximated as $\hat{\omega}(k)\hat{\omega}(k)^\top \leq \hat{\Upsilon}$, where $\hat{\Upsilon} = \hat{q}\,\mathrm{diag}(\hat{\omega}_{1,\max}^2, \ldots, \hat{\omega}_{\hat{q},\max}^2) \in \mathbb{R}^{\hat{q}\times\hat{q}}$ is a positive-definite matrix.

Based on Assumption 3 and the assumption that the dimensions n_o, n_c, p, and m are known, we can employ Algorithm 1 to design an RDPC scheme for the system (76).

We first collect multiple IO trajectories of the system (70) under the disturbance $\nu_{j,[0,T_j-1]}$ and the measurement noise $\delta_{y,j,[0,T_j]}$ satisfying Assumption 3, denoted as $(u_{j,[0,T_j-1]}, y_{j,[0,T_j-1]})$, $j = 1,\ldots,r$. For each trajectory $j \in \mathscr{R}$, we define the following data matrices:

$$\hat{X}_j = [\hat{x}(\bar{n}), \hat{x}(\bar{n}+1), \ldots, \hat{x}(T_j-1)] \tag{77a}$$

$$\hat{X}_{j,+} = [\hat{x}(\bar{n}+1), \hat{x}(\bar{n}+2), \ldots, \hat{x}(T_j)] \tag{77b}$$

$$\hat{U}_j = [u(\bar{n}), u(\bar{n}+1), \ldots, u(T_j-1)] \tag{77c}$$

$$\hat{Y}_j = [y(\bar{n}), y(\bar{n}+1), \ldots, y(T_j-1)] \tag{77d}$$

where $\bar{n} = \max(n_o, n_c)$.

Let $\hat{A} \in \mathbb{R}^{\hat{n}\times\hat{n}}$, $\hat{B} \in \mathbb{R}^{\hat{n}\times m}$, $\hat{C} \in \mathbb{R}^{p\times\hat{n}}$, and $\hat{D} \in \mathbb{R}^{p\times m}$ represent all possible system matrices in (76) that are capable of generating the precollected data $(u_{j,[0,T_j-1]}, y_{j,[0,T_j-1]})$ $\forall j \in \mathscr{R}$. Following a similar process to Section III-A, we construct an intersection set that contains all possible system matrices $\hat{A}$, $\hat{B}$, $\hat{C}$, and $\hat{D}$ as

$$\hat{\Sigma}^\star = \bigcap_{j=1}^{r} \hat{\Sigma}_j \tag{78}$$

where $\hat{\Sigma}_j = \{(\hat{A}, \hat{B}, \hat{C}, \hat{D}) | [I_{\hat{n}+p+m}, \hat{Z}] \hat{N}_j [I_{\hat{n}+p+m}, \hat{Z}]^\top \leq 0\}$ with

$$\begin{aligned}\hat{Z} &= \begin{bmatrix} \hat{A}^\top & (Q^{\frac{1}{2}}\hat{C})^\top & 0 \\ \hat{B}^\top & (Q^{\frac{1}{2}}\hat{D})^\top & R^{\frac{1}{2}} \end{bmatrix}^\top \\ \hat{N}_j &= \hat{H}_j \hat{H}_j^\top - \hat{\mathcal{G}} \hat{\Upsilon}_{T_j} \hat{\mathcal{G}}^\top \text{ with } \hat{\Upsilon}_{T_j} = (T_j - \bar{n})\hat{\Upsilon} \\ \hat{H}_j &= [\hat{X}_{j,+}^\top, (Q^{\frac{1}{2}}\hat{Y}_j)^\top, (R^{\frac{1}{2}}\hat{U}_j)^\top, -\hat{X}_j^\top, -\hat{U}_j^\top]^\top \\ \hat{\mathcal{G}} &= \begin{bmatrix} \hat{\mathcal{E}}_t^\top & Q^{\frac{1}{2}} & 0_{p\times m} & 0 & 0_{p\times m} \\ E_{1t}^\top & (Q^{\frac{1}{2}}G_{1t})^\top & 0 & -E_{2t}^\top & 0 \end{bmatrix}^\top \\ G_{1t} &= [0_{p\times n_o p}, I_p].\end{aligned} \tag{79}$$

Similarly, we define the intersection set containing all possible row vectors $\hat{C}_\iota$ and $\hat{D}_\iota$, where $\hat{C}_\iota$ and $\hat{D}_\iota$ are the ιth rows of $\hat{C}$ and $\hat{D}$, respectively

$$\hat{\Sigma}_{y_\iota}^\star = \bigcap_{j=1}^{r} \hat{\Sigma}_{j,y_\iota} \quad \forall \iota \in \mathscr{P} \tag{80}$$

where $\hat{\Sigma}_{j,y_\iota} = \{(\hat{C}_\iota, \hat{D}_\iota) | [1, \hat{Z}_\iota] \hat{N}_{j,y_\iota} [1, \hat{Z}_\iota]^\top \leq 0\}$ with $\hat{Z}_\iota = [\hat{C}_\iota, \hat{D}_\iota]$, and $\hat{N}_{j,y_\iota} = \hat{H}_{j,y_\iota} \hat{H}_{j,y_\iota}^\top - \hat{\mathcal{G}}_{y_\iota} \hat{\Upsilon}_{T_j} \hat{\mathcal{G}}_{y_\iota}^\top$. Here, $\hat{H}_{j,y_\iota} = [\hat{Y}_{j,\iota}^\top, -\hat{X}_j^\top, -\hat{U}_j^\top]^\top$ with $\hat{Y}_{j,\iota}$ being the ιth row of $\hat{Y}_j$, and

$$\mathcal{G}_{y_\iota} = \begin{bmatrix} e_\iota^\top & 0 & 0_{p\times m} \\ G_{1,\iota}^\top & -E_{2t}^\top & 0 \end{bmatrix}^\top$$

with $G_{1,\iota}$ and e_ι being the ιth rows of G_{1t} and I_p, respectively.

Then, similar to the problem (26), an optimization problem can be formulated using the sets (78) and (80). If this newly formulated problem is feasible at the time $k = \bar{n}$, an RDPC

Authorized licensed use limited to: University of Science & Technology of China. Downloaded on October 13,2025 at 10:47:17 UTC from IEEE Xplore. Restrictions apply.

scheme can be designed for the system (76) by iteratively solving it.

Moreover, since $\hat{B}_t$ and $\hat{D}_t$ are known from (74) and (75), they can be used to refine the sets $\hat{\Sigma}^\star$ and $\hat{\Sigma}^\star_{y_\iota}$, reducing conservativeness in the controller design. To achieve this, we construct the following data matrices:

$$\hat{\mathcal{X}} = 0_{\hat{n}\times m}, \hat{\mathcal{X}}_+ = \hat{B}_t, \hat{\mathcal{U}} = I_m, \hat{\mathcal{Y}} = \hat{D}_t$$

which satisfy

$$\hat{\mathcal{X}}_+ = \hat{A}\hat{\mathcal{X}} + \hat{B}\hat{\mathcal{U}} \tag{81a}$$

$$\hat{\mathcal{Y}} = \hat{C}\hat{\mathcal{X}} + \hat{D}\hat{\mathcal{U}} \tag{81b}$$

implying $\hat{B} = \hat{B}_t$ and $\hat{D} = \hat{D}_t$. Similar to (14)–(16), (81) is equivalent to

$$[I_{\hat{n}+p+m}, \hat{Z}]\hat{H}_{BD} = 0 \tag{82}$$

where $\hat{H}_{BD} = [\hat{B}_t^\top, (Q^{\frac{1}{2}}\hat{D}_t)^\top, (R^{\frac{1}{2}})^\top, 0_{m\times\hat{n}}, -I_m]^\top$.

Right-multiplying both sides of (82) by its transpose yields

$$[I_{\hat{n}+p+m}, \hat{Z}]\hat{N}_{BD}[I_{\hat{n}+p+m}, \hat{Z}]^\top = 0 \tag{83}$$

where $\hat{N}_{BD} = \hat{H}_{BD}\hat{H}_{BD}^\top$. Since for any real matrix Ψ, the condition $\Psi\Psi^\top = 0$ implies $\Psi = 0$, it follows that (83) is equivalent to (82), and thus to (81). This uniquely determines $\hat{B}$ and $\hat{D}$ as $\hat{B} = \hat{B}_t$ and $\hat{D} = \hat{D}_t$. Consequently, define the set

$$\hat{\Sigma}_{BD} = \{(\hat{A}, \hat{B}, \hat{C}, \hat{D}) | (83) \text{ holds}\}$$

which uniquely contains $\hat{B}$ and $\hat{D}$. A refined system set is then given by

$$\hat{\Sigma}^\star_{BD} = \hat{\Sigma}^\star \cap \hat{\Sigma}_{BD}$$

which is a subset of $\hat{\Sigma}^\star$ and contains uniquely $\hat{B}$ and $\hat{D}$.

Similarly, define the set for $(\hat{C}_\iota, \hat{D}_\iota)\ \forall \iota \in \mathscr{P}$, as

$$\hat{\Sigma}^\star_{y_\iota,D} = \hat{\Sigma}^\star_{y_\iota} \cap \hat{\Sigma}_D \tag{84}$$

where $\hat{\Sigma}_D = \{(\hat{C}_\iota, \hat{D}_\iota) | [1, \hat{Z}_\iota]\hat{N}_{y_\iota,D}[1, \hat{Z}_\iota]^\top = 0\}$ with $\hat{N}_{y_\iota,D} = \hat{H}_{y_\iota,D}\hat{H}_{y_\iota,D}^\top$ and $\hat{H}_{y_\iota,D} = [0_{m\times(\hat{n}+1)}, -I_m]^\top$.

Using the intersection sets $\hat{\Sigma}^\star_{BD}$ and $\hat{\Sigma}^\star_{y_\iota,D}\ \forall \iota \in \mathscr{P}$, we formulate a constrained RDPC scheme for the system (76). Analogous to Theorems 1 and 2, we establish the following corollary.

Corollary 1: Consider the system (76) [i.e., the system (70) with the output measurement noise] subject to the input and output constraints (24a) and (24b). Suppose that Assumption 3 holds and that n_o, n_c, p, and m are known. Given a group of sets of precollected IO data $(u_{j,[0,T_j-1]}, y_{j,[0,T_j-1]})\ \forall j \in \mathscr{R}$ of (76) and a positive constant γ, if there exist scalars $\bar{\eta}_k > \Delta\eta$ with $\Delta\eta = L\gamma^2\|\hat{\Upsilon}\|_2$, $\bar{\alpha}_{j,k} \geq 0$, $\bar{\beta}_k > 0$, $\tau_{j,\iota,k} \geq 0$, and $\lambda_{\iota,k} > 0 \forall j \in \mathscr{R} \cup \{0\}$ and $\iota \in \mathscr{P}$, a matrix $\bar{S}_k \in \mathbb{R}^{m\times\hat{n}}$, and a positive-definite matrix $\bar{\Gamma}_k \in \mathbb{R}^{\hat{n}\times\hat{n}}$ such that the following optimization problem (85) is feasible at time k:

$$\min_{\substack{\bar{\eta}_k, \bar{\alpha}_{j,k}, \bar{\beta}_k, \bar{S}_k, \\ \bar{\Gamma}_k, \tau_{j,\iota,k}, \lambda_{\iota,k}, \\ \forall \iota \in \mathscr{P} \quad \forall j \in \mathscr{R}\cup\{0\}}} \bar{\eta}_k \tag{85a}$$

s.t.

$$(26b), (26d) \tag{85b}$$

$$\bar{\mathcal{M}}_k - \bar{\alpha}_{0,k}\hat{\mathcal{N}}_{BD} - \sum_{j=1}^{r}\bar{\alpha}_{j,k}\hat{\mathcal{N}}_j \leq \begin{bmatrix} -\bar{\beta}_k I & 0 \\ 0 & 0 \end{bmatrix} \tag{85c}$$

$$\bar{\mathcal{M}}_{y_\iota,k} - \tau_{0,\iota,k}\hat{\mathcal{N}}_{y_\iota,D} - \sum_{j=1}^{r}\tau_{j,\iota,k}\hat{\mathcal{N}}_{j,y_\iota} \leq \begin{bmatrix} -\lambda_{\iota,k} & 0 \\ 0 & 0 \end{bmatrix}$$

$$\forall \iota \in \mathscr{P} \tag{85d}$$

Algorithm 2: Constrained RDPC Scheme With IO Data.

Data: Input-output sequences

Choose a positive scalar γ;

Initialize $k = \bar{n}$;

loop

  Construct $\hat{x}(k)$ using the past n_c-step inputs and n_o-step outputs;

  Set $\hat{x}(k|k) = \hat{x}(k)$ and solve (85);

  Compute $\hat{F}_k = \bar{S}_k\bar{\Gamma}_k^{-1}$;

  Apply the control input $u(k|k) = \hat{F}_k\hat{x}(k|k)$;

  Collect the output measurement $y(k)$;

  Update $k = k + 1$;

end loop

then $\hat{x}(k|k)^\top\bar{\eta}_k\bar{\Gamma}_k^{-1}\hat{x}(k|k) + L\gamma^2\|\hat{\Upsilon}\|_2$ is an upper bound on $J(k)$; the dynamic output feedback controller $u(k) = \hat{F}_k\hat{x}(k)$ with $\hat{F}_k = \bar{S}_k\bar{\Gamma}_k^{-1}$ minimizes this bound; and the predicted inputs and outputs satisfy the constraints (28a) and (28b) for all $i = 0, \ldots, L-1$, respectively. Here, $\hat{\mathcal{N}}_j = \mathrm{diag}(\hat{N}_j, 0)$ with $\hat{N}_j$ being defined in (79); $\hat{\mathcal{N}}_{BD} = \mathrm{diag}(\hat{N}_{BD}, 0)$ with $\hat{N}_{BD}$ being defined right after (83); $\hat{\mathcal{N}}_{j,y_\iota} = \mathrm{diag}(\hat{N}_{j,y_\iota}, 0)$ with $\hat{N}_{j,y_\iota}$ being defined right after (80); and $\hat{\mathcal{N}}_{y_\iota,D} = \mathrm{diag}(\hat{N}_{y_\iota,D}, 0)$ with $\hat{N}_{y_\iota,D}$ being defined right after (84). Matrices $\tilde{E}$, $\tilde{G}$, and $\bar{\mathcal{R}}_k$ in $\bar{\mathcal{M}}_k$ and $\bar{\mathcal{M}}_{y_\iota,k}$ are defined as $\tilde{E} = [\hat{\mathcal{E}}_t, I_{\hat{n}}]\mathcal{L}_1$, $\tilde{G} = [I_p, 0_{p\times(\hat{n}-p)}, I_p]\mathcal{L}_1$, and

$$\bar{\mathcal{R}}_k = \begin{bmatrix} \bar{\Gamma}_k + \frac{1}{\gamma^2}\bar{\eta}_k\mathcal{L}_2\mathcal{L}_2^\top & \bar{S}_k^\top & 0 \\ \bar{S}_k & 0 & \bar{S}_k \\ 0 & \bar{S}_k^\top & -\bar{\Gamma}_k \end{bmatrix}.$$

Furthermore, if (85) is feasible at $k = \bar{n}$, then the following holds:

1) it remains feasible for all $k \in \mathbb{N}^+$;
2) if $\hat{\omega}(k) = 0$, the system output converges to zero under the controller $u(k) = \hat{F}_k\hat{x}(k)$;
3) if $\hat{\omega}(k) \neq 0$, the closed-loop system with $\hat{x}(\bar{n}) = 0$ has the H_∞ performance

$$\sum_{k=\bar{n}}^{T}\|z(k)\|_2^2 \leq \gamma^2\sum_{k=\bar{n}}^{T}\|\hat{\omega}(k)\|_2^2$$

for all $\hat{\omega}(k) \in \mathcal{L}_2[0, T]$.

The proof of Corollary 1 follows from Theorems 1 and 2 and is omitted for brevity. The proposed constrained RDPC scheme using IO data is summarized in Algorithm 2.

Remark 19: This section focuses solely on the IO properties of systems with unmeasurable states. The proposed approach

Authorized licensed use limited to: University of Science & Technology of China. Downloaded on October 13,2025 at 10:47:17 UTC from IEEE Xplore. Restrictions apply.

does not rely on estimating the actual system state but instead constructs a new state $\hat{x}(k)$ in (72) only using past inputs and outputs. This constructed state serves as the basis for designing a dynamic output feedback controller at each time step k, ensuring that the system output converges to zero in the absence of disturbances and satisfies the prescribed H_∞ performance criteria when disturbances are present. Importantly, this differs fundamentally from a standard observer [41], which estimates the actual system state. Consequently, the proposed approach does not require the system to be observable. However, to guarantee the internal stability of the closed-loop system in the absence of disturbances, properties, such as detectability, are needed. In addition, similar to the input sequence in Section III, the method proposed here does not require the input sequence to satisfy the PE condition.

Remark 20: This section formulates the problem using an ARX model (70), aligning it structurally with system (6) to leverage the theoretical framework developed in Section III. The transformation from (72) to (80) is nontrivial and requires careful derivation. Notably, in the resulting state-space model (76), the system matrices $\hat{B}_t$ and $\hat{D}_t$ are known, distinguishing it from (6). Leveraging these known matrices, we introduce novel techniques to further refine the constructed system set, thereby reducing conservativeness. This necessitates a distinct optimization problem (85), which differs from (26) as presented in Theorem 1.

V. Case Study

This section demonstrates the effectiveness of the proposed methods by utilizing an unstable batch reactor [42]. The system is discretized with a sampling time of 0.1 s [43], yielding the following discrete-time state-space model:

$$x_t(k+1) = A_t x_t(k) + B_t u(k) + \omega_d(k) \tag{86a}$$

$$y_t(k) = C_t x_t(k) \tag{86b}$$

where $u(k) \in \mathbb{R}^2$ is the system input, $x_t(k) \in \mathbb{R}^4$ is the system state, $y_t(k) \in \mathbb{R}^2$ is the system output, and $\omega_d(k) \in \mathbb{R}^4$ represents the disturbance. The system matrices are given by

$$A_t = \begin{bmatrix} 1.178 & 0.002 & 0.512 & -0.403 \\ -0.052 & 0.662 & -0.011 & 0.061 \\ 0.076 & 0.335 & 0.561 & 0.382 \\ -0.001 & 0.335 & 0.089 & 0.849 \end{bmatrix}$$

$$B_t = \begin{bmatrix} 0.005 & -0.088 \\ 0.467 & 0.001 \\ 0.213 & -0.235 \\ 0.213 & -0.016 \end{bmatrix}, C_t = \begin{bmatrix} 1 & 0 & 1 & -1 \\ 0 & 1 & 0 & 0 \end{bmatrix}.$$

These matrices are assumed to be unknown and are only used for simulating the system. We assume that the state and output measurements are subject to noise $\delta_x(k) \in \mathbb{R}^4$ and $\delta_y(k) \in \mathbb{R}^2$, respectively, with each entry of $\omega_d(k)$, $\delta_x(k)$, and $\delta_y(k)$ bounded by $[-0.01, 0.01]$. The input and output constraints are set as $|u_\iota(k)| \leq 2$ and $|y_\iota(k)| \leq 1$ for all $\iota = 1, 2$.

We consider two cases. In the first case, we assume that the state is measurable and implement the constrained RDPC scheme using ISO data (see Algorithm 1). In the second case, we assume that the state is unmeasurable and apply the RDPC scheme using IO data (see Algorithm 2). For comparison, we also simulate the RMPC scheme from [3] in the first case and the RDMPC scheme from [13] in the second case. All control schemes use identical weight matrices, $Q = 10I_2$ and $R = I_2$, with a prediction horizon of $L = 6$. The initial state is set as $x_0 = [0.40, 0.30, 0.15, 0.08]^\top$. The simulations were carried out on a laptop equipped with an Intel Core i7-10875H CPU @ 2.30 GHz, 16 GB of memory, and running Windows 11 Enterprise.

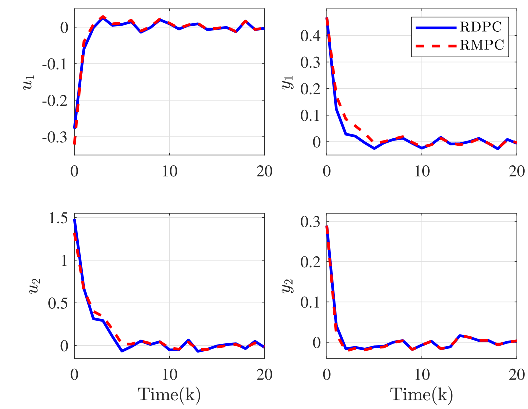

Fig. 1. Closed-loop input and output responses under RDPC and RMPC [3].

TABLE I
Total Costs and Iteration Time for RDPC and RMPC

Methods	RDPC	RMPC
$\bar{J}_1$	6.2186	6.1045
$\mathcal{I}_t$ (s)	0.0273	0.0047

We first examine the scenario where the state is measurable and compare the proposed RDPC scheme with the RMPC scheme from [3], under identical disturbances and measurement noise.

The system disturbance is defined as $\omega(k) = [\omega_d(k)^\top, \delta_y(k)^\top, \delta_x(k+1)^\top, \delta_x(k)^\top]^\top$, yielding $E_t = [I_4, 0_{4\times 2}, I_4, -A_t]$ and $G_t = [0_{2\times 4}, I_2, 0_{2\times 4}, -C_t]$. This formulation ensures that the system follows the general structure of (6). To implement the RDPC scheme with multiple datasets (see Algorithm 1), we first collect 15 ISO trajectories of length $T_\jmath = 1$, denoted as $(u_{\jmath,[0,0]}, x_{\jmath,[0,1]}, y_{\jmath,[0,0]})$ for $\jmath = 1, \ldots, 15$, with input values randomly selected from $[-2, 2]$. The collected data do not satisfy the PE condition of 10 required by the RDMPC scheme [13]. According to Remark 4, we generate 1940 datasets of length not exceeding 4. From these, we select all datasets of length 1 and randomly choose five datasets of length 2–4, respectively. The attenuation level is set to $\gamma = 30$. Notably, using a single ISO trajectory of length 15 directly would render the problem (26) in Algorithm 1 infeasible.

The simulation results for system input and output are depicted in Fig. 1. The solid blue lines correspond to the proposed RDPC scheme, while the red dashed lines represent the RMPC scheme. Both approaches achieve the control target. However, our method attains comparable performance to the RMPC scheme without requiring information on the system matrices but only utilizing the collected data. The total simulation cost, defined as $\bar{J}_1 = \sum_{k=0}^{20} y(k)^\top Q y(k) + u(k)^\top R u(k)$, is presented in Table I. The results indicate that the RDPC

Authorized licensed use limited to: University of Science & Technology of China. Downloaded on October 13,2025 at 10:47:17 UTC from IEEE Xplore. Restrictions apply.

scheme achieves a cost very close to that of the RMPC scheme, further demonstrating its effectiveness, i.e., our method achieves comparable control performance to the RMPC scheme by only utilizing the collected data.

Table I also presents the average computation time per iteration, $\mathcal{I}_t$, for both methods. The RMPC scheme has a lower computational cost since it is designed based on a known nominal system model. In contrast, the RDPC scheme requires additional computation to construct the system set from historical IO data, leading to higher computational complexity. While the RMPC benefits from its reliance on a predefined model, the RDPC offers greater flexibility by operating solely on data. Reducing the computational burden of the RDPC is an important direction for future research.

Subsequently, we consider the case where the state is unmeasurable and compare the proposed RDPC scheme (see Algorithm 2) with the RDMPC scheme [13]. Since the RDMPC scheme accounts for measurement noise $\omega_n(k)$ but does not consider disturbances $\omega_d(k)$, we ensure a fair comparison by assuming that the system (86) is only affected by noise, i.e., $\omega_d(k) = 0$. According to [44], the IO behavior of (86) under this assumption can be represented by the ARX model (70) with $n_o = n_c = 2$ and $\nu(k) = 0$. Defining $\hat{\omega}(k) = [\delta_y(k-2)^\top, \delta_y(k-1)^\top, \delta_y(k)^\top]^\top$, we apply Algorithm 2 to design an RDPC scheme for (86) with $\omega_d(k) = 0$.

According to [13], for an RDMPC scheme with a prediction horizon of $L = 6$, the theoretical minimum precollected data length is $T = 41$. However, our simulations indicate that the RDMPC scheme does not achieve the control objective for $T = 41$, and the shortest practical data length that enables successful control is $T = 43$. For improved performance, we also simulate the case for $T = 48$. The precollected data used for the RDMPC scheme are denoted as $(u_{[0,47]}, y_{[0,47]})$. For the RDMPC scheme with multiple datasets, the theoretical minimum length of a single trajectory is 14, and the corresponding minimum total length of all trajectories is $T = 54$.

In Algorithm 2, we set $\gamma = 300$. In addition, we consider only the IO constraints of the nominal system, aligning with the RDMPC scheme. Under this assumption, where the system (6) operates without disturbances (i.e., $\omega(k) = 0$), we directly set $\Delta\eta = 0$ in (26b), based on the proof of Theorem 1. The RDPC scheme utilizes the first 32 data points from the precollected RDMPC dataset, i.e., $(u_{[0,31]}, y_{[0,31]})$.

Following (77a)–(77d), we extract 30 datasets of length one, defined as $\hat{X}^j = \hat{x}(j+1)$, $\hat{X}^j_+ = \hat{x}(j+2)$, $\hat{Y}^j = y(j+1)$, and $\hat{U}^j = u(j+1)$, for $j = 1, \ldots, 30$, where $\hat{x}(j) = [u(j-2)^\top, u(j-1)^\top, y(j-2)^\top, y(j-1)^\top]^\top$. According to Remark 4, we generate 31 930 additional datasets of length not exceeding 4. As in the first case, we select all datasets of length 1 and randomly choose ten datasets of lengths 2–4.

The simulation results for system input and output are shown in Fig. 2. The solid blue lines represent the results of the proposed constrained RDPC scheme, while the red and green dashed lines correspond to the RDMPC scheme with different precollected data lengths. All schemes achieve the control objective. Notably, the RDPC scheme with $T = 32$ achieves comparable performance to the RDMPC scheme with $T = 48$ and outperforms the RDMPC scheme with $T = 43$.

The total cost incurred over the simulation period, defined as $\bar{J}_2 = \sum_{k=0}^{30} y(k)^\top Q y(k) + u(k)^\top R u(k)$, is presented in Table II. The results are consistent with Fig. 2, where the RDPC scheme achieves a similar cost to the RDMPC scheme with $T = 48$ and outperforms the RDMPC scheme with $T = 43$. These findings highlight that the proposed method achieves comparable control performance to the RDMPC scheme while requiring less precollected data.

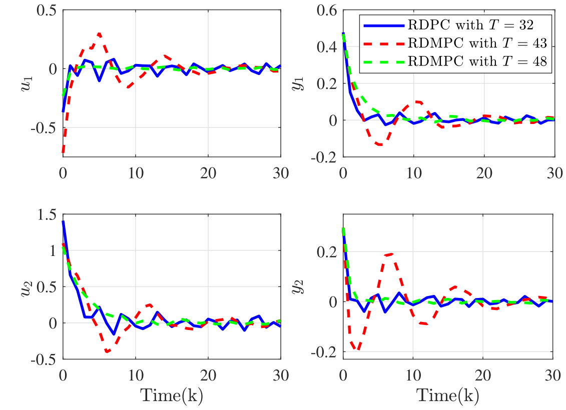

Fig. 2. Closed-loop input and output responses under RDPC and RDMPC [13].

TABLE II
TOTAL COSTS AND ITERATION TIME FOR RDPC AND RDMPC

Method	RDPC ($T = 32$)	RDMPC ($T = 43$)	RDMPC ($T = 48$)
$\bar{J}_2$	6.5461	10.3209	6.5054
$\mathcal{I}_t$ (s)	0.0981	0.6952	1.9211

Regarding the average computation time per iteration, $\mathcal{I}_t$, for the RDPC scheme and the RDMPC scheme, Table II also gives that the RDPC scheme demonstrates a lower computational burden compared to the RDMPC scheme with both $T = 43$ and $T = 48$, further supporting its efficiency.

VI. CONCLUSION

This article presented an RDPC framework for LTI systems affected by bounded disturbances and measurement noise. Recognizing that disturbances and noise introduce ambiguity in system identification, we constructed a set of all possible systems consistent with the collected ISO data, ensuring that the true system is included. This set was formulated using QMIs, which formed the basis for designing the RDPC scheme using multiple datasets. Furthermore, we extended the proposed control framework to scenarios where the system state is unmeasurable, leveraging an ARX model to reformulate the problem in an IO setting. This extension broadens the applicability of the method to practical systems where direct state measurement is not feasible. The effectiveness of the proposed approach was validated through a case study on an unstable batch reactor.

REFERENCES

[1] S. V. Raković and W. S. Levine, *Handbook of Model Predictive Control*, Cham, Switzerland: Springer 2018.

[2] A. Bemporad and M. Morari, “Robust model predictive control: A survey,” in *Robustness in Identification and Control*. New York, NY, USA: Springer-Verlag, 1999, pp. 207–226.

[3] D. Mayne, M. Seron, and S. Raković, “Robust model predictive control of constrained linear systems with bounded disturbances,” *Automatica*, vol. 41, no. 2, pp. 219–224, 2005.

Authorized licensed use limited to: University of Science & Technology of China. Downloaded on October 13,2025 at 10:47:17 UTC from IEEE Xplore. Restrictions apply.

[4] D. Q. Mayne, E. C. Kerrigan, E. J. van Wyk, and P. Falugi, "Tube-based robust nonlinear model predictive control," *Int. J. Robust Nonlinear Control*, vol. 21, no. 11, pp. 1341–1353, 2011.
[5] F. Y. Taşçikaraoglu, L. Ucun, and I. B. Küçükdemiral, "Receding horizon H_∞ control of time-delay systems," *Trans. Inst. Meas. Control*, vol. 37, no. 5, pp. 596–605, 2015.
[6] M. V. Kothare, V. Balakrishnan, and M. Morari, "Robust constrained model predictive control using linear matrix inequalities," *Automatica*, vol. 32, no. 10, pp. 1361–1379, 1996.
[7] T. Basar, "A dynamic games approach to controller design: Disturbance rejection in discrete-time," *IEEE Trans. Autom. Control*, vol. 36, no. 8, pp. 936–952, Aug. 1991.
[8] A. Tangirala, *Principles of System Identification: Theory and Practice*, Boca Raton, FL, USA: CRC Press, 2015.
[9] C. D. Persis and P. Tesi, "Formulas for data-driven control: Stabilization, optimality, and robustness," *IEEE Trans. Autom. Control*, vol. 65, no. 3, pp. 909–924, Mar. 2020.
[10] K. Hu and T. Liu, "Data-driven H_∞ control for unknown linear time-invariant systems with bounded disturbances," in *Proc. IEEE Conf. Decis. Control*, 2022, pp. 1423–1428.
[11] S. Moschoyiannis, E. Chatzaroulas, V. Šliogeris, and Y. Wu, "Deep reinforcement learning for stabilization of large-scale probabilistic Boolean networks," *IEEE Trans. Control Netw. Syst.*, vol. 10, no. 3, pp. 1412–1423, Sep. 2023.
[12] J. Coulson, J. Lygeros, and F. Dörfler, "Data-enabled predictive control: In the shallows of the DeePC," in *Proc. Eur. Control Conf.*, 2019, pp. 307–312.
[13] J. Berberich, J. Köhler, M. A. Müller, and F. Allgöwer, "Data-driven model predictive control with stability and robustness guarantees," *IEEE Trans. Autom. Control*, vol. 66, no. 4, pp. 1702–1717, Apr. 2021.
[14] J. Coulson, J. Lygeros, and F. Dörfler, "Regularized and distributionally robust data-enabled predictive control," in *Proc. IEEE Conf. Decis. Control*, 2019, pp. 2696–2701.
[15] K. Zhang, Y. Zheng, C. Shang, and Z. Li, "Dimension reduction for efficient data-enabled predictive control," *IEEE Control Syst. Lett.*, vol. 7, pp. 3277–3282, 2023.
[16] L. Huang, J. Coulson, J. Lygeros, and F. Dörfler, "Decentralized data-enabled predictive control for power system oscillation damping," *IEEE Trans. Control Syst. Technol.*, vol. 30, no. 3, pp. 1065–1077, May 2022.
[17] P. G. Carlet, A. Favato, R. Torchio, F. Toso, S. Bolognani, and F. Dörfler, "Real-time feasibility of data-driven predictive control for synchronous motor drives," *IEEE Trans. Power Electron.*, vol. 38, no. 2, pp. 1672–1682, Feb. 2023.
[18] J. C. Willems, P. Rapisarda, I. Markovsky, and B. D. Moor, "A note on persistency of excitation," *Syst. Control Lett.*, vol. 54, no. 4, pp. 325–329, 2005.
[19] S. Talebi, S. Alemzadeh, N. Rahimi, and M. Mesbahi, "On regularizability and its application to online control of unstable LTI systems," *IEEE Trans. Autom. Control*, vol. 67, no. 12, pp. 6413–6428, Dec. 2022.
[20] H. J. van Waarde, C. D. Persis, M. K. Camlibel, and P. Tesi, "Willems' fundamental lemma for state-space systems and its extension to multiple datasets," *IEEE Control Syst. Lett.*, vol. 4, no. 3, pp. 602–607, Jul. 2020.
[21] M. Alsalti, M. Barkey, V. G. Lopez, and M. A. Müller, "Sample- and computationally efficient data-driven predictive control," in *Proc. Eur. Control Conf.*, Stockholm, Sweden, 2024, pp. 84–89.
[22] H. J. van Waarde, J. Eising, H. L. Trentelman, and M. K. Camlibel, "Data informativity: A new perspective on data-driven analysis and control," *IEEE Trans. Autom. Control*, vol. 65, no. 11, pp. 4753–4768, Nov. 2020.
[23] H. J. van Waarde, M. K. Camlibel, and M. Mesbahi, "From noisy data to feedback controllers: Nonconservative design via a matrix S-lemma," *IEEE Trans. Autom. Control*, vol. 67, no. 1, pp. 162–175, Jan. 2022.
[24] H. J. van Waarde, M. K. Camlibel, J. Eising, and H. L. Trentelman, "Quadratic matrix inequalities with applications to data-based control," *SIAM J. Control Optim.*, vol. 61, no. 4, pp. 2251–2281, 2023.
[25] T. R. V. Steentjes, M. Lazar, and P. M. J. Van den Hof, "On data-driven control: Informativity of noisy input-output data with cross-covariance bounds," *IEEE Control Syst. Lett.*, vol. 6, pp. 2192–2197, 2022.
[26] H. H. Nguyen, M. Friedel, and R. Findeisen, "LMI-based data-driven robust model predictive control," *IFAC-PapersOnLine*, vol. 56, no. 2, pp. 4783–4788, 2023.
[27] Y. Xie, J. Berberich, and F. Allgower, "Data-driven min-max MPC for linear systems," in *Proc. Amer. Control Conf.*, Toronto, Canada, 2024, pp. 3184–3189.
[28] K. Hu and T. Liu, "Robust data-driven predictive control for unknown linear time-invariant systems," *Syst. Control Lett.*, vol. 193, 2024, Art. no. 105914.
[29] F. L. Lewis and K. G. Vamvoudakis, "Reinforcement learning for partially observable dynamic processes: Adaptive dynamic programming using measured output data," *IEEE Trans. Syst., Man, Cybern., Part B (Cybernetics)*, vol. 41, no. 1, pp. 14–25, Feb. 2011.
[30] K. Hu and T. Liu, "Data-driven output-feedback control for unknown switched linear systems," *IEEE Control Syst. Lett.*, vol. 7, pp. 2299–2304, 2023.
[31] S. P. Boyd, *Convex Optimization*. Cambridge, U.K.: Cambridge Univ. Press, 2004.
[32] B. Kouvaritakis and M. Cannon, *Model Predictive Control: Classical, Robust and Stochastic*. Cham, Switzerland: Springer, 2016.
[33] D. Mayne, S. Raković, R. Findeisen, and F. Allgöwer, "Robust output feedback model predictive control of constrained linear systems," *Automatica*, vol. 42, no. 7, pp. 1217–1222, 2006.
[34] F. Zhang, *The Schur Complement and Its Applications*, New York, NY, USA: Springer Science, 2005.
[35] A. Bisoffi, L. Li, C. D. Persis, and N. Monshizadeh, "Controller synthesis for input-state data with measurement errors," *IEEE Control Syst. Lett.*, vol. 8, pp. 1571-1576, 2024.
[36] K. Hu and T. Liu, "A robust data-driven iterative control method for linear systems with bounded disturbances," 2024, *arXiv:2405.02537*.
[37] A. Alanwar, Y. Stürz, and K. H. Johansson, "Robust data-driven predictive control using reachability analysis," *Eur. J. Control*, vol. 68, 2022, Art. no. 100666.
[38] W. Kühn, "Rigorously computed orbits of dynamical systems without the wrapping effect," *Computing*, (Vienna/New York), vol. 61, no. 1, pp. 47–67, 1998.
[39] H. Kong, M. Shan, S. Sukkarieh, T. Chen, and W. X. Zheng, "Kalman filtering under unknown inputs and norm constraints," *Automatica*, vol. 133, 2021, Art. no. 109871.
[40] S. Bolognani, R. Carli, G. Cavraro, and S. Zampieri, "Distributed reactive power feedback control for voltage regulation and loss minimization," *IEEE Trans. Autom. Control*, vol. 60, no. 4, pp. 966–981, Apr. 2015.
[41] P. J. Antsaklis and A. N. Michel, *A Linear Systems Primer*. Boston, Mass: Birkhäuser, 2007.
[42] G. C. Walsh and H. Ye, "Scheduling of networked control systems," *IEEE Control Syst. Mag.*, vol. 21, no. 1, pp. 57–65, Feb. 2001.
[43] W. Liu, J. Sun, G. Wang, F. Bullo, and J. Chen, "Data-driven resilient predictive control under denial-of-service," *IEEE Trans. Autom. Control*, vol. 68, no. 8, pp. 4722–4737, Aug. 2023.
[44] I. Markovsky and P. Rapisarda, "Data-driven simulation and control," *Int. J. Control*, vol. 81, no. 12, pp. 1946–1959, 2008.

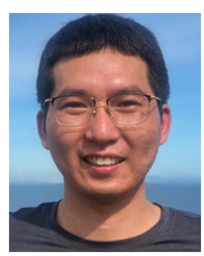

Kaijian Hu received the B.Eng. degree in automation from the Liaoning University of Science and Technology, Anshan, China, in 2014, and the M.Eng. degree in control theory and control engineering from the Dalian University of Technology, Dalian, China, in 2017. He is currently working toward the Ph.D. degree in control theory with the Department of Electrical and Electronic Engineering, The University of Hong Kong, Hong Kong.

His research interests include data-driven control, model predictive control, and unmanned aerial vehicle control.

Tao Liu (Member, IEEE) received the B.E. degree in automation from Northeastern University, Shenyang, China, in 2003, and the Ph.D. degree in engineering from Australian National University (ANU), Canberra, ACT, Australia, in 2011.

From 2012 to 2015, he worked as a Postdoctoral Fellow with ANU, University of Groningen, and The University of Hong Kong (HKU). He became a Research Assistant Professor at HKU in 2015 and is currently an Assistant Professor. His research interests include power system analysis and control, data-driven control, distributed control/optimization, event-triggered control, and complex dynamical networks.

Authorized licensed use limited to: University of Science & Technology of China. Downloaded on October 13,2025 at 10:47:17 UTC from IEEE Xplore. Restrictions apply.